

# Interaction of Ibuprofen with Partially Unfolded Bovine Serum Albumin in the Presence of Ionic Micelles and Oligosaccharides at Different $\lambda_{ex}$ and pH: A Spectroscopic Analysis

Debasish Rout, Shweta Sharma, Pratibha Agarwala, Arun K. Upadhyaya, Akanksha Sharma, and Dibyendu K. Sasmal\*



Cite This: *ACS Omega* 2023, 8, 3114–3128



Read Online

ACCESS |

Metrics & More

Article Recommendations

Supporting Information

**ABSTRACT:** The interaction between the plasma protein bovine serum albumin (BSA) and the drug ibuprofen (IBU) has been investigated at three different pH values (7.4, 6.5, and 8.0) in the presence of oligosaccharides and surfactants. The interaction analysis of BSA with oligosaccharides and surfactants has also been studied in the absence of the drug ibuprofen. The results obtained give convenient and efficient access to understand the mechanism of binding of ibuprofen to BSA, and the major forces involved are found to be hydrophobic forces, hydrogen bonding and ionic interactions. In addition to that, the formation of inclusion complexes of ibuprofen with oligosaccharides ( $\beta$ -CD and 2-HP- $\beta$ -CD) has been observed, which has depicted that due to the hydrophobic nature of ibuprofen, it becomes more soluble in the presence of oligosaccharides, but due to the larger size of the inclusion complexes, these could not be able to access the hydrophobic pocket of BSA where tryptophan-212 (Trp-212) resides. The binding interaction between BSA and ibuprofen is observed in the presence of surfactants (SDS and CTAB), which partially unfold the protein. Non-radiative fluorescence resonance energy transfer (FRET) from Trp and Tyr residues of BSA in the presence of an anionic surfactant SDS to ibuprofen has depicted that there is a possibility of drug binding even in the partially unfolded state of BSA protein. Furthermore, the distance between the protein and the drug has been calculated from the FRET efficiency, which gives a comprehensive overview of ibuprofen binding to BSA even in its partially denatured state. The hydrophobic drug binding to the partially unfolded serum albumin protein (BSA) supports the “necklace and bead structures” model and opens up a new direction of drug loading and delivery system, which will have critical therapeutic applications in the efficient delivery of pharmacologically prominent drugs.



## 1. INTRODUCTION

Over the years, plasma proteins, especially serum albumins (SAs), and their interaction analysis with drugs have received tremendous attention due to their applicability in understanding the pharmacodynamic and pharmacokinetic properties of drugs.<sup>1–3</sup> Moreover, reversibility of binding, binding forces, binding sites, and conformational changes in the protein upon drug binding provides insights into the mechanism of interaction and also plays a significant role in pharmaceutically important drug designing and delivery.<sup>4–6</sup> Bovine serum albumin (BSA) is a globular protein<sup>7</sup> found predominantly in the circulatory system of cows having a molecular weight of ~66.5 kDa. Its primary structure consists of 583 amino acids and 17 cysteine residues which are connected by 8 disulfide bridges, and there is one free thiol group.<sup>8</sup> At pH 7, the net charge on BSA is found to be  $-18$ .<sup>9</sup> It belongs to the class of SAs which are considered the most important plasma proteins as they play pivotal roles in drug delivery due to their ability to reversibly bind to therapeutic molecules and act as carriers for various fatty acids, amino acids, bile salts, metal ions,

hormones, and drugs.<sup>10</sup> The secondary structure of BSA consists of 67%  $\alpha$ -helix and 10% turn configurations without any  $\beta$ -sheets, while its tertiary structure is composed of three domains (I, II, and III), and each consists of two subdomains (A and B).<sup>11</sup> BSA is structurally homologous to protein human serum albumin (HSA), both of which are alike in terms of ligand binding affinity and share almost 80% sequence homology.<sup>12</sup> There are two tryptophan (Trp) residues present in BSA, Trp-134 and Trp-212; Trp-134 is located on the surface of domain IB, whereas Trp-212 is located in the hydrophobic pocket of subdomain IIA; thus, the micro-environment around Trp-134 is more polar than that around

**Received:** October 5, 2022

**Accepted:** December 8, 2022

**Published:** January 10, 2023



Trp-212.<sup>13</sup> In addition to that, there are 19 tyrosine (Tyr) and 27 phenylalanine (Phe) residues in BSA.<sup>14</sup> Due to the photophysical properties of fluorescent amino acid residues, it is widely recognized that when the proteins are irradiated with an excitation wavelength of 275 nm, it leads to the excitation of both Trp and Tyr residues, but at 295 nm, there is no absorption of Tyr residues, so it only excites Trp-212.<sup>15</sup> Despite being a complex protein, the structure and dynamics of BSA can be investigated by the use of the intrinsic fluorescence shown by Trp amino acid residues.<sup>16</sup> Among various SAs, which are medically important, of low cost, and easily available and having unusual ligand binding properties, and analogy with HSA, BSA is widely selected as a model protein for extensive study.<sup>17</sup> Ibuprofen belongs to a class of drugs popularly called non-steroidal anti-inflammatory drugs (NSAIDs), which are approved by the Food and Drug Administration (FDA) to be used as an anti-inflammatory, antipyretic, and analgesic medication.<sup>18</sup> NSAIDs are mainly categorized into different groups based on their chemical composition and selectivity, namely, acetylated salicylates, fenamates, alkanones, acetic acid derivatives, propionic acid derivatives, sulfonanilides, enolic acid derivatives, and diaryl heterocyclic.<sup>19</sup> Among these, ibuprofen is the first member of the propionic acid derivative group. Like most NSAIDs, ibuprofen is non-selective, and its mechanism of action is to inhibit the enzyme prostaglandin-endoperoxide synthase (PTGS) [also called cyclooxygenase (COX)], which leads to the inhibition of prostaglandin synthesis.<sup>20</sup> It has two enantiomeric forms, R(−)-ibuprofen and S(+)-ibuprofen, and only the S(+)-enantiomer can inhibit COX.<sup>21</sup> Ibuprofen is one of the most commonly used medications, available in the form of oral tablets, and is used to treat fever and reduce pain (migraines, muscle aches, toothache, period pain, etc.) and inflammation.<sup>22</sup> The important therapeutic applications of ibuprofen are to cure patent ductus arteriosus (PDA), rheumatoid arthritis (RA), osteoarthritis (OA), orthostatic hypotension, dysmenorrhea, cystic fibrosis, and breast cancer. Still, clinical trials are going on to study its therapeutic effect on deadly diseases such as Alzheimer's disease and Parkinson's disease, and also among the conventional NSAIDs, ibuprofen is rated as the safest drug by the spontaneous adverse drug reaction reporting system in the United Kingdom.<sup>23</sup> The diversified applications and effectiveness of ibuprofen make it a proper candidate for detailed investigation and analysis of its mechanism of binding and interaction with SA proteins, which act as depot and transport proteins.

In the current study, we have used two cyclic oligosaccharides,  $\beta$ -cyclodextrin ( $\beta$ -CD) and (2-hydroxypropyl)- $\beta$ -cyclodextrin (2-HP- $\beta$ -CD), to enhance the solubility, stability, and bioavailability<sup>24</sup> of the hydrophobic drug ibuprofen as these macrocyclic molecules have a unique shape like truncated cones, having an inner non-polar surface and an outer polar surface which help them to form inclusion complexes<sup>25</sup> and hence to improve the drug delivery.<sup>26</sup> 2-HP- $\beta$ -CD has improved water solubility as compared to  $\beta$ -CD<sup>27</sup> as it is a partially substituted polyhydroxypropyl ether of  $\beta$ -CD.<sup>28</sup>

Surface-active agents (surfactants) play pivotal roles in developing many pharmaceutical products and designing their delivery system<sup>29</sup> due to their unique amphiphilic nature which is attributed to their specialized structure having a distinct polar head and non-polar tail(s) region.<sup>30</sup> Here, we used one cationic surfactant cetyltrimethylammonium bromide (CTAB) and one anionic surfactant sodium dodecyl sulfate (SDS) to

investigate their effect on protein conformation and drug loading. In water, the critical micellar concentration (CMC) of CTAB and SDS is reported to vary between 0.9 and 1.0 mM and 8.0 and 8.20 mM, respectively.<sup>31</sup>

Conventionally, protein–drug interaction studies are carried out in vitro under physiological conditions, but in the present study, the effect of pH, the presence of oligosaccharides ( $\beta$ -CD and 2-HP- $\beta$ -CD) and surfactants (SDS and CTAB) on the binding interaction mechanism, polarity changes in the microenvironment of the protein, and secondary structural changes in the protein upon drug binding have been studied for the SA protein BSA and the NSAID ibuprofen by using molecular docking, UV–visible absorption analysis, fluorescence emission study, synchronous fluorescence spectroscopy (SFS), three-dimensional (3D) fluorescence, <sup>1</sup>H NMR, and circular dichroism (CD) spectroscopic analysis. In addition to that, we have performed a FRET experiment in the presence of surfactants to study the drug binding in the partially unfolded conformation of BSA. The data accumulated demonstrate the binding mechanism of BSA–ibuprofen interaction and can be extended to elucidate the mechanism of other hydrophobic NSAIDs with BSA and its structural homology HSA. The surfactants have been widely used to enhance the drug delivery by significantly enhancing the aqueous solubility and bioavailability of the hydrophobic drugs (like ibuprofen). Also, the release of the dissolved ibuprofen at very high concentrations of the surfactants will play a crucial role in efficient drug delivery and disease treatment.<sup>32,33</sup> Furthermore, hydrophobic drug binding to protein in the denatured protein conformation as demonstrated by FRET analysis directs an innovative way of drug binding, and the technique has convincing potential to be used as a convenient and efficient drug delivery technique for therapeutically important drugs.

## 2. EXPERIMENTAL SECTION

**2.1. Reagents.** BSA, potassium dihydrogen phosphate (KH<sub>2</sub>PO<sub>4</sub>), dipotassium hydrogen phosphate (K<sub>2</sub>HPO<sub>4</sub>), and deuterium oxide (D<sub>2</sub>O) 99.9 atom % D were purchased from Sigma-Aldrich (USA) and used directly without further purification. Tris-(hydroxymethyl) aminomethane (Tris–HCl), *N,N*-dimethylformamide (DMF), CTAB, SDS, beta-cyclodextrin ( $\beta$ -CD), and 2-hydroxypropyl beta-cyclodextrin (2-HP- $\beta$ -CD) were purchased from Fisher Scientific (India). Ibuprofen (4-isobutyl- $\alpha$ -methylphenylacetic acid, 99%) was purchased from Alfa Aesar. BSA and all other solutions were prepared in tris buffer for all UV–visible and fluorescence experiments and in PBS buffer for NMR experiments, respectively, unless otherwise mentioned and the pHs of the solutions were maintained by HCl and KOH. Milli-Q water was used for the preparation of all the solutions.

**2.2. UV–vis Absorption Spectroscopy.** UV–vis spectroscopic measurements were done using a LabIndia-2000U UV/vis spectrophotometer using a quartz cuvette of path length 1 cm. All the absorption spectra were recorded in the range of 200–500 nm at the normal response mode. The concentration of BSA was determined spectrophotometrically and was maintained at 25  $\mu$ M for each set of experiments. The absorbance data of BSA in the presence of surfactants, oligosaccharides, and ibuprofen were recorded every time, after equilibration of solutions for 5 min. In all the UV–visible absorption measurements, tris buffer was used as the reference solution.

**2.3. Fluorescence Spectroscopy.** Fluorescence emission spectra measurements were done by using a JASCO spectrofluorometer FP-8300 with a quartz cuvette of path length 1 cm. Two different excitation wavelengths  $\lambda_{\text{ex}} = 275$  and 295 nm were used, and the corresponding emission spectra were recorded in the range of 285–500 nm and 300–500 nm, respectively, at a scan speed of 1000 nm/min in very low sensitivity. The excitation and emission bandwidths were set at 5 nm, and the response time was 50 ms. Three sets of experiments were performed: (1) 25  $\mu\text{M}$  BSA with different concentrations of ibuprofen at three different pHs 6.5, 7.4, and 8. For each pH, six different solutions were prepared in which the BSA concentration was maintained at 25  $\mu\text{M}$ , and ibuprofen concentrations were varied from 0 to 100  $\mu\text{M}$ ; (2) 25  $\mu\text{M}$  BSA with different concentrations of surfactants (CTAB and SDS) in the absence and presence of 25  $\mu\text{M}$  ibuprofen at pH 7.4. BSA (25  $\mu\text{M}$ ) and different concentrations of CTAB and SDS solutions from 0 to 15 mM were prepared from stock solutions of 50  $\mu\text{M}$  BSA and 30 mM CTAB and SDS. For the preparation of BSA-surfactant solutions in the presence of the drug ibuprofen, 7.5 mM stock solution of ibuprofen was used. (3) BSA (25  $\mu\text{M}$ ) with different concentrations of oligosaccharides ( $\beta$ -CD and 2-HP- $\beta$ -CD) in the absence and presence of 25  $\mu\text{M}$  ibuprofen at pH 7.4. BSA (25  $\mu\text{M}$ ) and different concentrations of  $\beta$ -CD and 2-HP- $\beta$ -CD solutions from 0 to 10 mM were prepared by the addition of 1.7 and 2.3 mg of solid  $\beta$ -CD and 2-HP- $\beta$ -CD, respectively, in the same cuvette subsequently.

**2.4. Nuclear Magnetic Resonance Spectroscopy.** All  $^1\text{H}$  NMR experiments were performed on a Bruker High Performance Digital FT-NMR (Model: Advance III HD, Ascend™ WB, 500 MHz) at 25 °C using a probe tuned at 500 MHz. Phosphate-buffered saline (PBS) of concentration 0.2 M was prepared by dissolving a desired amount of  $\text{K}_2\text{HSO}_4$  and  $\text{KH}_2\text{SO}_4$  in water.  $\text{D}_2\text{O}$  was added to it to make 10%  $\text{D}_2\text{O}$  for the NMR spectrometer field-frequency lock. To enhance the solubility of the hydrophobic drug ibuprofen, few drops of 0.2 M *N,N*-dimethylformamide (DMF) were added into the buffer before sample preparation. The above-prepared buffer solution was used for the preparation of NMR sample solutions of ibuprofen (25 mM) and 25 mM ibuprofen with 0.25 mM BSA. Phase-shift pre-saturation was used to suppress the water signal.

**2.5. Synchronous Fluorescence Spectroscopy.** The same samples were used to record the SFS where the emission and excitation wavelengths were scanned simultaneously, and the scanning interval was individually fixed at  $\Delta\lambda = 15, 60$  nm to study the spectroscopic behaviors of tyrosine (Tyr) and tryptophan (Trp) residues of BSA, respectively. SFS were also recorded at  $\Delta\lambda = 35$  nm to distinguish between the fluorescence spectra of BSA and ibuprofen. For recording SFS at  $\Delta\lambda = 35$  nm, samples were prepared separately. The SFS data for all the experiments were recorded in the range of 300–500 nm.

**2.6. Circular Dichroism Spectroscopy.** CD spectroscopic measurements were done by a JASCO J-815 spectrophotometer (Japan spectroscopic company) equipped with a quartz cuvette of path length 1 cm. CD spectra were recorded in the range of 250–195 nm with a scanning speed of 100 nm/min in the continuous scanning mode at standard sensitivity and a bandwidth of 1 nm. The data pitch and digital integration time (DIT) were set at 0.5 nm and 1 s, respectively. All the spectra were baseline-corrected, and the final plot was

obtained from two accumulated plots. Here, two sets of experiments were performed—(1) BSA with different concentrations of ibuprofen at three different pHs 6.5, 7.4, and 8.0. For each pH, three different solutions were prepared in which the BSA concentration was maintained at 1  $\mu\text{M}$ , and ibuprofen concentrations were varied from 1 to 4  $\mu\text{M}$ . (2) BSA (1  $\mu\text{M}$ ) with CTAB and SDS (concentrations varied from 0 to 10 mM for both surfactants) in the presence and absence of 1  $\mu\text{M}$  ibuprofen. The corresponding  $\theta$  (in mdeg) obtained were then converted to respective mean residue ellipticity (MRE) (in deg  $\text{cm}^2 \text{dmol}^{-1}$ ) by using the formula

$$\text{MRE} = \frac{\text{Observed CD (in mdeg)}}{(C_p \times n \times l \times 10)} \quad (1)$$

where  $C_p$  = concentration of BSA,  $n$  = number of amino acid residues in the protein, and  $l$  = path length of the cuvette.

**2.7. 3-Dimensional Fluorescence Spectroscopy.** 3D fluorescence spectra were recorded at excitation and emission wavelength ranges from 225 to 325 nm and 235 to 500 nm, respectively, with a scan speed of 20,000 nm/min and a response time of 10 ms at very low sensitivity. The excitation and emission bandwidths are set at 10 nm. 3D contour plots were obtained for three different sets of solutions—(1) 25  $\mu\text{M}$  BSA with and without 15  $\mu\text{M}$  ibuprofen, (2) 25  $\mu\text{M}$  BSA with 40 mM SDS in the presence and absence of 15  $\mu\text{M}$  ibuprofen, and (3) 25  $\mu\text{M}$  BSA with 40 mM CTAB in the presence and absence of 15  $\mu\text{M}$  ibuprofen. The emission wavelengths (in nm) obtained for each plot were converted into corresponding emission energy (in eV) by the formula

$$E = \frac{hc}{\lambda} \quad (2)$$

where  $E$  = emission energy,  $h$  = Planck's constant ( $6.62607004 \times 10^{-34}$  J s) and  $c$  = velocity of light ( $3 \times 10^8$  m  $\text{s}^{-1}$ ).

**2.8. Förster Resonance Energy Transfer.** Förster resonance energy transfer (FRET) measurements were done at excitation wavelength  $\lambda_{\text{ex}} = 275$  nm, and emission data were recorded in the range of 285–500 nm. For the FRET study, 25  $\mu\text{M}$  BSA in the presence of 40 mM SDS (donor) and 10  $\mu\text{M}$  ibuprofen (acceptor) at pH = 7.4 were prepared. The efficiency of energy transfer and overlap integral  $J(\lambda)$  with respect to the acceptor followed by the actual distance between the donor and acceptor were calculated.

According to Förster's theory, the energy-transfer efficiency ( $E$ ) depends on the inverse of the sixth power of intermolecular separation distance calculated as follows

$$E = \frac{R_0^6}{(R_0^6 - r^6)} = \frac{|F_0 - F|}{F_0} \quad (3)$$

where  $F_0$  and  $F$  are the acceptor fluorescence intensities in the absence and presence of the donor, respectively, " $r$ " is the actual distance between the donor and acceptor, and  $R_0$  is the distance between the donor and acceptor at which 50% of the excitation energy is transmitted from the donor to the acceptor. To get the positive value of rise in the acceptor intensity, a modulus of  $(F_0 - F)$ , that is,  $|F_0 - F|$ , is taken.  $R_0$  is given by the equation

$$R_0 = \{8.79 \times 10^{-25} \times K^2 \times n^{-4} \times \Phi \times J(\lambda)\}^{1/6} \quad (4)$$

where  $K^2$  is the orientation factor related to the geometry of donor and acceptor, and its value lies between 0 and 2 and for

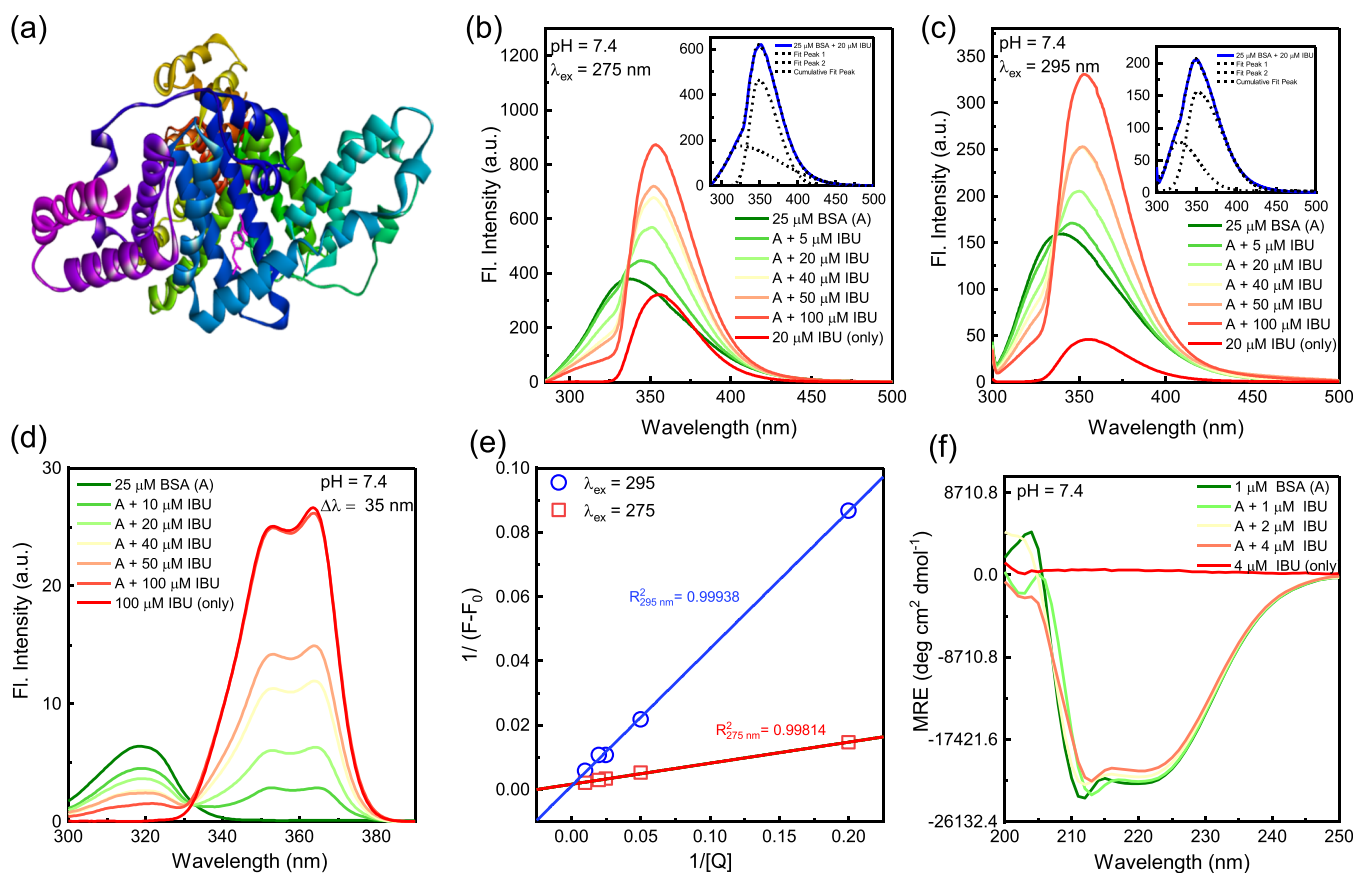


**Figure 1.** Binding interaction study of BSA and ibuprofen at pH = 7.4. (a) Energy-minimized conformation of BSA (PDB ID: 3V03) complexed with ibuprofen. The binding energy is obtained to be  $-7.29$  kcal/mol. (b,c) Fluorescence emission spectra of BSA at  $\lambda_{\text{ex}} = 275$  and  $295$  nm, respectively, in the presence of different concentration of ibuprofen from  $5$  to  $100$   $\mu\text{M}$ . The bent in the emission curve at around  $330$  nm is due to the resultant emission curve of fluorescent BSA and ibuprofen. The insets in respective plots show that theoretical splitting of the resultant curve into two subset peaks at  $320$  nm corresponds to BSA, and the peak at  $348$  nm corresponds to ibuprofen emission. (d) SFS at  $\lambda = 35$  nm of BSA at different concentrations of ibuprofen. The peak at  $318$  nm (corresponds to BSA) decreases, and two peaks at  $364$  and  $353$  nm (correspond to ibuprofen) increase as the concentration of ibuprofen varies from  $10$   $\mu\text{M}$  to  $10$ IM. (e) Represents Benesi–Hildebrand plots for  $\lambda_{\text{ex}} = 275$  and  $295$  nm, and their respective binding constants are  $K = 2.52 \times 10^4 \text{ M}^{-1}$  and  $K = 2.55 \times 10^3 \text{ M}^{-1}$ . (f) CD spectra of BSA at different concentrations of ibuprofen. The minima at  $\lambda = 208$  nm decreases as the concentration of ibuprofen increases from  $1$  to  $4$   $\mu\text{M}$ , which indicates the decrease of BSA  $\alpha$ -helix content from  $67.75$  to  $60.13\%$ . See Figures S1–S3 for interaction of BSA and ibuprofen at pH =  $6.5$  and  $8$ .

liquid solution  $K^2 = 2/3$ . For water, refractive index,  $n = 1.333$ ,  $\Phi$  is the quantum yield of the donor (BSA), and  $J(\lambda)$  is the degree of spectral overlap between donor emission spectra (BSA + SDS) and acceptor absorption spectra (ibuprofen) and is calculated by integrating the spectral overlap area.

The expression for  $J(\lambda)$  is calculated by

$$J(\lambda) = \frac{\int_0^\infty F(\lambda) \cdot \epsilon(\lambda) \cdot \lambda^4 \, d\lambda}{\int_0^\infty F(\lambda) \, d\lambda} \quad (5)$$

where  $F(\lambda)$  indicates the fluorescence intensity of the donor at the wavelength  $\lambda$  and  $\epsilon$  represents the molar absorption coefficient ( $\text{M}^{-1} \text{cm}^{-1}$ ) of the acceptor at wavelength  $\lambda$ .<sup>34</sup> The average value of  $r$  should lie in the range of  $0.5 R_0 < r < 1.5 R_0$ , which indicates whether the energy transfer from the donor to the acceptor is possible or not.

**2.9. Molecular Docking Analysis.** A molecular docking study was carried out by Autodock Tools 4.2 to calculate the binding affinity and binding energy of ibuprofen to BSA. The 3D crystal structure of protein BSA (PDB ID: 3V03) was downloaded from the RCSB Protein Data Bank (<http://www.rcsb.org>), and the ibuprofen structure was accessed from the

NCBI PubChem (<http://pubchem.ncbi.nlm.nih.gov/>) database. Open Babel software was used to convert the ligand from SMILE format to .pdb format. The polar hydrogens of the protein BSA were checked, and partial atomic charges were assigned. The rotatable bonds of the ligand ibuprofen were selected and defined. The grid box of dimension  $126 \times 126 \times 126$  points along the  $x$ ,  $y$ , and  $z$  directions, respectively, having coordinates of central grid point of maps ( $38.088$ ,  $22.672$ , and  $40.738$ ) with a grid spacing of  $0.375$   $\text{\AA}$  was generated to include the protein's binding pockets where the binding cavity was located. The minimum and maximum coordinates in grid are ( $14.463$ ,  $-0.953$ , and  $17.113$ ) and ( $61.713$ ,  $46.297$ , and  $64.363$ ) respectively. Finally, docking calculations of rigid modified protein BSA and flexible ligand ibuprofen were performed using AutoDock Tools using the Lamarckian genetic algorithm with all default parameter settings. Finally, from the molecular docking results, the one with the highest negative binding energy was selected as the most favorable structure of the BSA–ibuprofen complex. The post-screening analyses were performed using BIOVIA Discovery Studio 2020.

### 3. RESULTS AND DISCUSSION

**3.1. Binding Interaction Study of BSA and Ibuprofen at Different pHs Reveals Strong Interactions of BSA and Ibuprofen:  $\lambda_{\text{ex}}$  Variation, SFS, CD Spectroscopy, and Molecular Docking.** To elucidate the mechanism of interaction of ibuprofen with BSA, the molecular docking analysis tool is employed. The results show nine different conformations of interaction. The best conformation having the highest binding affinity, that is,  $-7.29$  kcal/mol, is selected for further analysis (Figure 1a). Like other hydrophobic NSAIDs, ibuprofen is also found to bind to the hydrophobic site of Sudlow II located in subdomain IIIA of BSA (Figure 1a).<sup>35</sup>

Fluorescence spectroscopy is used to investigate the interaction between BSA and ibuprofen as it is one of the most reliable and efficient methods for studying protein–ligand interactions.<sup>36</sup> BSA shows a distinct fluorescence peak at 340 nm, whereas ibuprofen shows a peak at 355 nm when excited at  $\lambda_{\text{ex}} = 275$  and 295 nm (Figure 1b,c). The fluorescence at  $\lambda_{\text{ex}} = 275$  nm is mainly due to both Trp and Tyr residues, whereas fluorescence emission at  $\lambda_{\text{ex}} = 295$  nm originates from Trp residues only.<sup>37</sup> The fluorescence spectra of BSA at different concentrations of ibuprofen at pH = 7.4,  $\lambda_{\text{ex}} = 275$ , and 295 nm are shown in Figure 1b,c, respectively. With the increase in the successive concentration of ibuprofen, it has been observed that the peak at 340 nm (corresponding to BSA) gets quenched and blue-shifted and appeared as a bent in the resultant curve, whereas an additional peak at 350 nm appeared (corresponding to ibuprofen emission) and its intensity got enhanced and red-shifted. The change in the peak intensity of BSA with an increase in the concentration of ibuprofen is shown in Figure S1b. The remarkable quenching in BSA peak intensity on the addition of ibuprofen suggests that ibuprofen interacts with BSA, and the blue shift in BSA emission maxima could be attributed to an increase in hydrophobicity in the microenvironment of the protein due to the interaction of ibuprofen with Trp-212, which is located in the hydrophobic core of the protein. The resultant plots for 25  $\mu\text{M}$  BSA and 25  $\mu\text{M}$  ibuprofen at  $\lambda_{\text{ex}} = 275$  and 295 nm have been deconvoluted and are shown in the insets of the respective graphs in Figure 1b,c to theoretically distinguish the two peaks corresponding to BSA and ibuprofen using the bi-Gaussian peak function. To further support the fact that the bending in the resultant curve is due to the quenching of BSA fluorescence by ibuprofen, an additional experiment has been performed keeping the ibuprofen concentration constant at 10  $\mu\text{M}$  and increasing the BSA concentration from 0 to 100  $\mu\text{M}$  at pH = 7.4 and  $\lambda_{\text{ex}} = 295$  nm (Figure S1a), and it is observed that the peak at 340 nm corresponding to BSA emission is enhanced.

To study the microenvironment of amino acid (Trp and Tyr) residues and to further support the above explanation, constant wavelength SFS is employed.<sup>38,39</sup> The optimum  $\Delta\lambda$  value, which can clearly differentiate BSA and ibuprofen fluorescence emission, is found to be 35 nm. It is observed that at  $\Delta\lambda = 35$  nm, only BSA (25  $\mu\text{M}$ ) showed a fluorescence emission peak at 318 nm, whereas only ibuprofen (100  $\mu\text{M}$ ) showed two SFS emission peaks at 364 and 353 nm (Figure 1d). The blue shift in the maximum emission peak of SFS of BSA from normal fluorescence emission spectra is due to the fact that Stokes shift (for BSA  $\sim 60$  nm) is greater than  $\Delta\lambda$  value (35 nm) used in SFS, whereas for ibuprofen, the SFS

maximum emission peaks are red-shifted as compared to the normal fluorescence emission peak because the Stokes shift (for ibuprofen  $\sim 30$  nm<sup>40</sup>) is smaller than SFS  $\Delta\lambda$ . With the increase in the concentration of ibuprofen (from 0 to 100  $\mu\text{M}$ ), it is found that the peak at 318 nm (corresponding to BSA) is quenched, whereas the intensities of the two peaks at 353 and 364 nm (corresponding to ibuprofen) are enhanced. This observation further supports our explanation of the interaction of ibuprofen with BSA as observed in normal fluorescence emission. SFS data are also recorded at  $\Delta\lambda = 15$  and 60 nm to explore the change in the microenvironment of the amino acid residues Tyr and Trp, respectively.<sup>41–43</sup> SFS at  $\Delta\lambda = 15$  nm (Figure S1c) shows one peak at 302 nm for BSA only corresponding to Tyr emission. With the increase in the concentration of ibuprofen, the peak at 302 nm undergoes quenching, while an additional peak at 346 nm corresponding to ibuprofen intensity gets enhanced. This observation suggests that the binding of ibuprofen to BSA does not change the polarity around the microenvironment of the Tyr residues, but there is the quenching of fluorescence intensity which is consistent with the fluorescence emission experiment. In contrast, at  $\Delta\lambda = 60$  nm (Figure S1d), only BSA shows a synchronous fluorescence peak at 339 nm corresponding to Trp emission. There is an overall increase in resultant peak intensity and appearance of additional peaks as well as a red shift is observed with an increase in ibuprofen concentration. The appearance of bent in the resultant emission plots at 339 nm and in addition of ibuprofen implies that there is quenching as well as a blue shift in Trp emission due to the binding of ibuprofen to BSA. Further, the blue shift suggests that due to the interaction of ibuprofen and BSA, there is an increase in hydrophobicity around the Trp microenvironment. The quenching in the synchronous fluorescence peak of BSA is consistent with the previous fluorescence experiment. A similar trend is observed in the synchronous plots ( $\Delta\lambda = 15$  and 60 nm) at pH = 6.5 and 8 (Figure S1i–l).

The mechanism of protein fluorescence quenching and enhancement in the presence of a drug is studied by using the Stern–Volmer equation and the Benesi–Hildebrand equation, respectively.<sup>42,44</sup> There is a decrease in the fluorescence intensity of BSA with the addition of ibuprofen, but there is an overall increase in resultant fluorescence intensity due to the addition of ibuprofen as it is itself fluorescent. Hence, the Benesi–Hildebrand equation is used to calculate the binding constant of the interaction of ibuprofen with BSA. The Benesi–Hildebrand equation is given by the formula

$$\frac{1}{(F - F_0)} = \frac{1}{(F' - F_0)K} \frac{1}{[Q]} + \frac{1}{(F' - F_0)} \quad (6)$$

where  $F$  = fluorescence intensity of protein in the presence of ibuprofen,  $F_0$  = fluorescence intensity of protein in the absence of ibuprofen,  $F'$  = fluorescence intensity of protein at the highest concentration of ibuprofen,  $[Q]$  = concentration of ibuprofen, and  $K$  = binding constant. Here, the binding constant ( $K$ ) is obtained by dividing the intercept by the slope of the graph  $1/(F - F_0)$  versus  $1/[Q]$ , that is

$$K = \frac{\text{Intercept}}{\text{Slope}} \quad (7)$$

The slope and intercept at  $\lambda_{\text{ex}} = 275$  and 295 nm are obtained to be 0.06555, 0.00165 and 0.42763, 0.00109, respectively. The binding constant ( $K$ ) is determined by eq

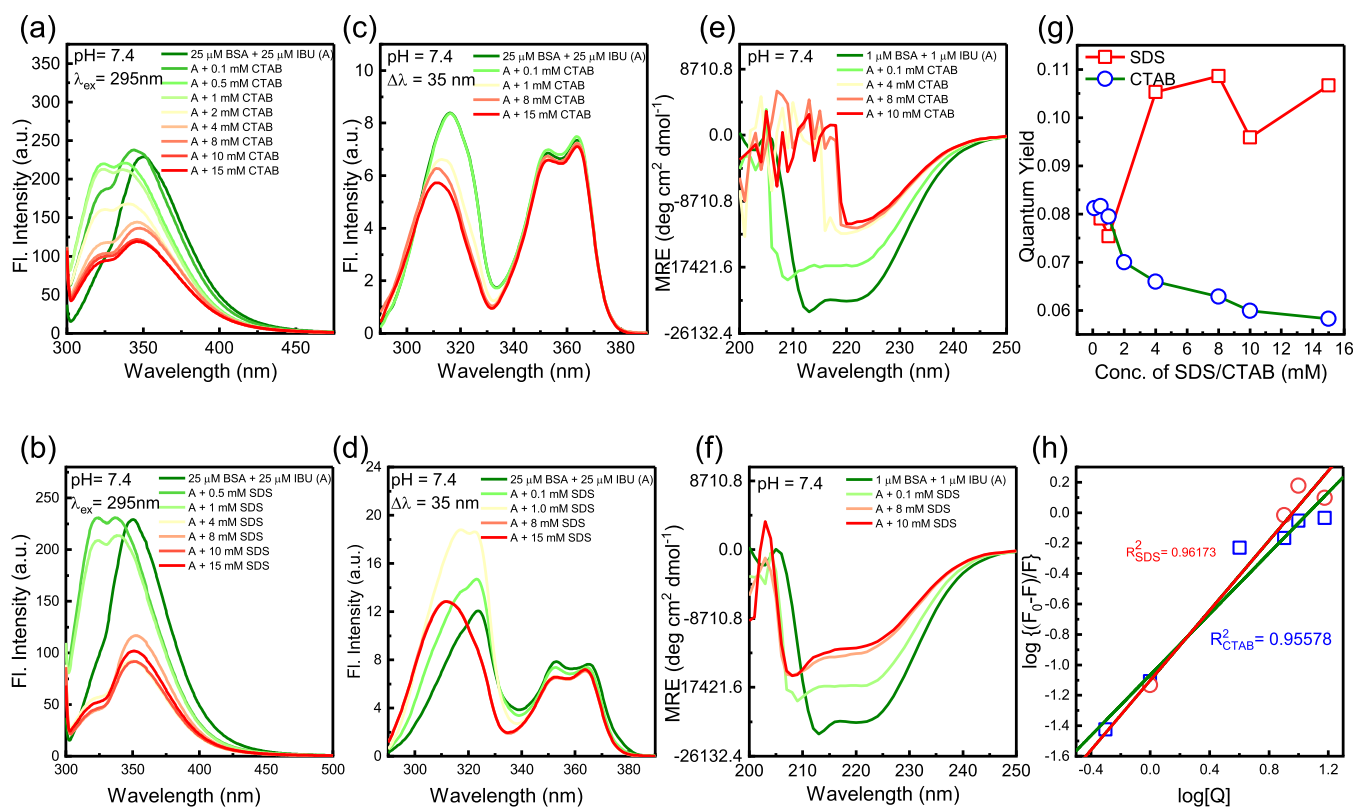


**Figure 2.** Interaction analysis of BSA and ibuprofen in the presence of surfactants gives inference of ibuprofen binding to BSA even in partially denatured conformation at pH = 7.4. (a,b) Fluorescence emission spectra of BSA and ibuprofen at different concentrations of CTAB and SDS, respectively, from 0.1 to 15 mM at  $\lambda_{\text{ex}} = 295$  nm. The blue shift of emission maxima with the addition of surfactants corresponds to an increase in hydrophobicity around the tryptophan residue before CMC (CTAB = 1 mM and SDS = 8 mM), and there is a decrease in fluorescence intensity and a red shift in fluorescence spectra after CMC, which corresponds to an increase in polarity around the tryptophan environment due to the unfolding of the protein by the surfactants. (c,d) SFS of BSA and ibuprofen at  $\Delta\lambda = 35$  nm in the presence of CTAB and SDS, respectively. The red shift in peak at 318 nm (corresponds to BSA) and the decrease in fluorescence intensity correspond to unfolding of the protein and increase in polarity around the microenvironment of the tryptophan and tyrosine residues. (e,f) CD spectra of BSA (1  $\mu\text{M}$ ) in the presence of ibuprofen (1  $\mu\text{M}$ ) at different concentrations from 0.1 to 10 mM of CTAB and SDS, respectively. The decrease in negative MRE value at  $\lambda = 208$  nm with the addition of surfactants corresponds to a decrease in the BSA  $\alpha$ -helix content from 67.19% at 0 mM CTAB to 47.43% at 0.1 mM concentration of CTAB (CMC of CTAB); then, the peak at 208 nm gets vanished at higher concentrations of CTAB. For SDS, the decrease in the  $\alpha$ -helix content is observed from 64.19% at 0 mM SDS to 38.43% at 10 mM SDS. (g) Quantum yield of BSA and ibuprofen in the presence of various concentrations of CTAB and SDS at  $\lambda_{\text{ex}} = 295$  nm. The quantum yield of BSA and ibuprofen remains nearly the same before CMC and then decreases with an increase in the concentration of CTAB above CMC, but the quantum yield at a lower concentration of SDS remains nearly the same; then, it increases and attains a constant value just before CMC and finally decreases above CMC. (h) Double-logarithm Stern–Volmer plots for BSA and ibuprofen in the presence of CTAB and SDS at  $\lambda_{\text{ex}} = 295$  nm. The number of binding sites in BSA complexed with ibuprofen for CTAB and SDS are obtained to be 0.99841 and 1.146, respectively.

7. The binding constants at  $\lambda_{\text{ex}} = 275$  and 295 nm are obtained to be  $2.52 \times 10^4$  and  $2.55 \times 10^3$   $\text{M}^{-1}$ . A higher binding constant at  $\lambda_{\text{ex}} = 275$  nm refers to the fact that at 275 nm, both Trp and Tyr residues get excited, while at 295 nm, only Trp gets excited.

To study the change in the secondary structure of BSA by the binding interaction of ibuprofen, the CD spectroscopic technique is used (Figure 1f).<sup>45</sup> It has been previously reported that BSA shows two characteristic negative minima at  $\lambda = 208$  and 222 nm corresponding to  $n \rightarrow \pi^*$  and  $\pi \rightarrow \pi^*$  transitions of the peptide bonds of  $\alpha$ -helix.<sup>46</sup> Also, the maximum  $\alpha$ -helix content of BSA is observed at pH = 7.4, that is, 67.75%,<sup>15</sup> which is nearly matching to the previously reported results.<sup>15,47,48</sup> It is observed that the  $\alpha$ -helix percentage of BSA decreases as the ibuprofen concentration increases from 0 to 2  $\mu\text{M}$  (Figure 1f), which is reflected in the mean residual ellipticity (MRE) versus wavelength plot as there is a decrease in MRE value observed at 222 nm with an increase in the

concentration of ibuprofen. This might be attributed to the fact that BSA undergoes complex formation with ibuprofen; as a result, there are certain conformational changes in the BSA secondary structure. The  $\alpha$ -helix percentage for only BSA (1  $\mu\text{M}$ ) is calculated to be 67.75%, which decreases to 60.13% on addition of ibuprofen (up to 4  $\mu\text{M}$ ). The conformational changes in the BSA secondary structure with different ibuprofen concentrations at pH = 6.5 and 8 are shown in Figure S3a,b. At pH 6.5 and 8, the  $\alpha$ -helix percentage of 1  $\mu\text{M}$  BSA is found to be 57.93 and 50.92% respectively, which on addition of ibuprofen (up to 4  $\mu\text{M}$ ) decreases to 56.8 and 49.57%, respectively. Notably, there is no significant change in the shape of the minima and their position due to addition of ibuprofen, indicating that there is no overall structural change of the protein by the interaction with ibuprofen.

The interaction of ibuprofen with BSA has further been investigated by using <sup>1</sup>H-proton nuclear magnetic resonance (NMR) spectroscopy (Figure S2). Only ibuprofen (25 mM)

shows eight peaks corresponding to eight different electronic microenvironments of protons. With the addition of 0.25 mM BSA, the proton peaks of ibuprofen undergo line broadening, quenching, and up-field chemical shift corresponding to interaction between BSA and ibuprofen. In principle, the circulation of electrons around the nucleus creates local magnetic fields, which generally opposes the external magnetic field and attribute to different chemical shifts.<sup>49</sup> The up-field drift of the chemical shift of ibuprofen upon addition of BSA implies that the protons of free and BSA-bound ibuprofen have different chemical shifts, and also the effective field experienced by the ibuprofen protons is decreased by binding with BSA.<sup>50</sup> The NMR signals of BSA are negligibly weak and are close to the baseline as the ratio of BSA to ibuprofen is taken as 1:100. The interaction of BSA and ibuprofen is also studied at pH = 6.5 and 8 at  $\lambda_{\text{ex}} = 275$  and 295 nm to study the effect of pH on the interaction of BSA and ibuprofen (Figure S1e–h). It has been observed that there is no significant effect on conformation change by pH (in the range of 6.5–8) on the binding interaction of ibuprofen and BSA as further proved by CD spectroscopy (Figures 1f and S3).

### 3.2. Interaction Analysis of BSA and Ibuprofen in the Presence of Surfactants Gives Inference of Ibuprofen Binding to BSA Even in Partially Denatured Conformation.

The mechanism of interaction between BSA and ibuprofen in the presence of varying concentrations of surfactants (CTAB and SDS) is studied by fluorescence spectroscopy at pH = 7.4 and  $\lambda_{\text{ex}} = 295$  nm (Figure 2a,b). It has been found that for only BSA and ibuprofen complex,  $\lambda_{\text{em}}$  is observed at 350 nm, on the addition of CTAB/SDS to the solution of BSA (25  $\mu\text{M}$ ) and ibuprofen (25  $\mu\text{M}$ ), the two peaks, which are not distinguished previously in 25  $\mu\text{M}$  BSA and 25  $\mu\text{M}$  ibuprofen solution, become prominent at 323 nm (corresponds to BSA in unfolded state) and 343 nm (corresponds to ibuprofen in the presence of CTAB/SDS). The above explanation is further supported by the blue shifting of the BSA peak from 340 to 310 nm and 340 to 323 nm by the addition of surfactants CTAB and SDS, respectively, in the absence of ibuprofen at  $\lambda_{\text{ex}} = 295$  nm as shown in Figure S4f,h at pH = 7.4, respectively.

To investigate the effect of surfactants on the binding interaction of ibuprofen to BSA and its effect on both Trp and Tyr residues of the protein, fluorescence emission is also recorded at  $\lambda_{\text{ex}} = 275$  nm (Figure S4a,b). Here, it is also observed that the BSA peak (at  $\lambda_{\text{ex}} = 320$  nm) corresponding to the emission of both Trp and Tyr residues starts getting prominent with the increase in the concentration of CTAB and SDS. For both cationic (CTAB) and anionic (SDS) surfactants, at  $\lambda_{\text{ex}} = 275$  and 295 nm, it is observed before CMC (0.1 mM for CTAB and 8 mM for SDS<sup>51</sup>) that the quenching in fluorescence intensities is small, but after CMC, the fluorescence intensity suddenly decreases. The trend is quite the same in the absence of the drug ibuprofen at  $\lambda_{\text{ex}} = 275$  and 295 nm (Figure S4e–h). Due to the strong electrostatic interaction between the cationic surfactant CTAB and negatively charged BSA at pH = 7.4, there is partial denaturation of the protein BSA, which might be responsible for increase in hydrophobicity around the tryptophan and tyrosine residues of BSA by the CTAB micelles and leading to a blue shift in the emission peak. For the anionic surfactant SDS also, a blue shift in emission maxima is observed on addition of SDS, but there is a decrease in fluorescence intensity before CMC. The possible reason

might be electrostatic repulsion between the anionic SDS surfactants and the negatively charged protein BSA, leading to weakening of the interaction between SDS and the Trp and Tyr residues, thereby only quenching of fluorescence emission is observed before CMC. However, after CMC, both cationic and anionic micelles of CTAB and SDS, respectively, interact with the Trp and Tyr residues of the protein; hence, sudden quenching in fluorescence emission peaks is observed. SFS (at  $\Delta\lambda = 35$  nm) is used to study the effect of surfactants on the microenvironment of protein BSA on binding to the drug ibuprofen. As shown in Figure 2c, there is a hypsochromic shift in the emission peak of BSA after CMC, that is, 0.1 mM for CTAB. The blue shift in the emission maxima of BSA after CMC might be due to an increase in hydrophobicity around the Trp and Tyr residues by the hydrophobic core of the micelle. The quenching in the fluorescence intensity of both BSA and ibuprofen is consistent with the previous fluorescence experimental data. For anionic surfactant SDS (Figure 2d) also, a similar trend is observed, that is, after CMC (8 mM), a sudden blue shift in emission maxima is observed, but before CMC, with the increase in the concentration of SDS, the intensity of the BSA peak increases. The possible reason might be the electrostatic attraction between the cationic surfactant and the negatively charged protein, leading to provide a hydrophobic environment to the outer Trp-134, whose fluorescence was previously quenched by the solvents.

To analyze the effect of surfactants in changing the microenvironment of Tyr and Trp residues of BSA, SFS data are also recorded at  $\Delta\lambda = 15$  and 60 nm, respectively (Figure S4i–l). SFS at  $\Delta\lambda = 15$  nm corresponding to Tyr emission get blue-shifted with the rise in the concentration of surfactants (both CTAB and SDS), but there is a non-uniform decrease and increase in SFS intensity observed (Figure S4j,k), whereas SFS at  $\Delta\lambda = 60$  nm corresponding to Trp emission shows an SFS peak at 339 nm, which gets blue-shifted on the addition of surfactants (for both CTAB and SDS), also the peak intensities get quenched (Figure S4j,l, respectively). The blue shift might be due to an increase in hydrophobicity around the microenvironment of Trp<sup>52</sup> residue, while the linear quenching of peak intensity for Trp emission is consistent with the fluorescence experimental data.

CD spectroscopic analysis is performed to study the change in the secondary structure of BSA when complexed with ibuprofen in the presence of surfactant (CTAB/SDS) (Figure 2e,f). It is found that an increase in the concentration of CTAB and SDS not only decreases the depth of the minima but also changes the position and shape of the minima (MRE). On addition of CTAB, after a concentration greater than 0.1 mM (CMC of CTAB), there is a rapid decrease in negative MRE value at  $\lambda = 208$  nm and the peak almost vanished, and there are consecutive negative and positive peaks, at higher CTAB concentrations, which is probably due to an extensive interaction between the positively charged CTAB micelles and BSA; as a result, most helical structures get disrupted.<sup>53</sup> On addition of the anionic surfactant SDS, it is observed that the  $\alpha$ -helix of BSA (1  $\mu\text{M}$ ) in the presence of ibuprofen (1  $\mu\text{M}$ ) decreases from 64.19 to 38.43% with the increase in the concentration of SDS from 0 to 10 mM. Changes in the secondary structure of BSA by the interaction with SDS and CTAB are also studied separately in the absence of ibuprofen (Figure S5a,b, respectively). The decrease in negative MRE value at  $\lambda = 208$  nm with the rise in the concentration of SDS or CTAB suggests that the  $\alpha$ -helix content of BSA decreases

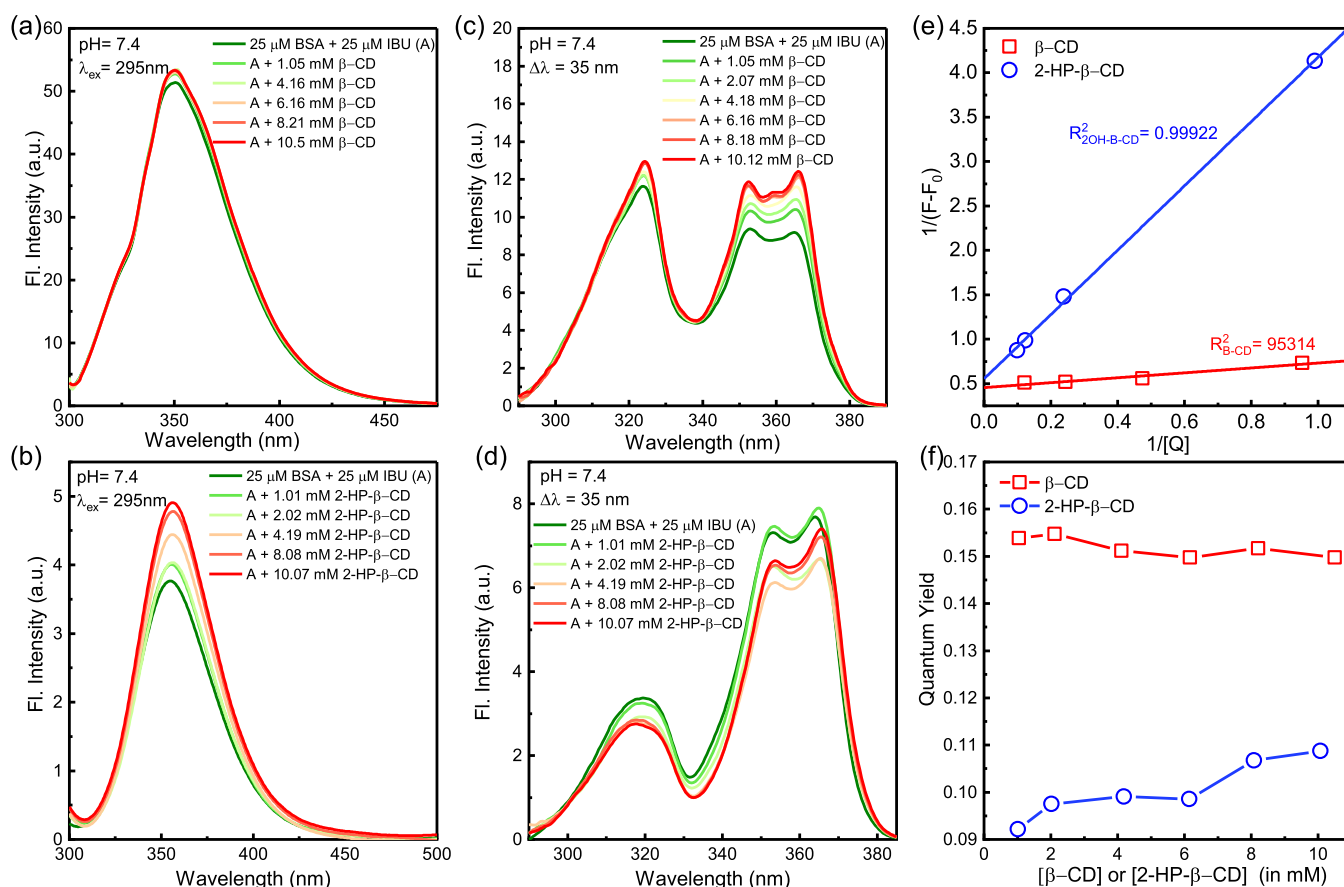


**Figure 3.** Presence of oligosaccharides ( $\beta$ -CD and 2-HP- $\beta$ -CD) decreases the ibuprofen binding to BSA but increases the solubility of hydrophobic drug ibuprofen by the formation of inclusion complex at pH = 7.4. (a,b) Represent the fluorescence emission spectra of BSA and ibuprofen at different concentrations of  $\beta$ -CD and 2HP- $\beta$ -CD, respectively, at  $\lambda_{ex} = 295$  nm. There is an increase in the fluorescence intensity peak of BSA and ibuprofen with an increase in the concentration of  $\beta$ -CD and 2HP- $\beta$ -CD (from 1 to 10 mM), but the increase is not much clearly indicates that there is not much interaction between tryptophan-213 and the oligosaccharides as they could not approach the hydrophobic core of the protein where Trp-213 resides, but these oligosaccharides form an inclusion complex with ibuprofen. (c,d) SFS of BSA and ibuprofen at  $\Delta\lambda = 35$  nm at different concentrations of  $\beta$ -CD and 2-HP- $\beta$ -CD. The peak at 318 nm (corresponds to BSA) decreases, but the decrease is not much and two peaks at 364 and 353 nm (corresponds to ibuprofen) show a non-linear behavior. (e) Stern–Volmer plots for BSA and ibuprofen in the presence of  $\beta$ -CD and  $K_{sv} = 1.65 \times 10^3$  M $^{-1}$  and 2HP- $\beta$ -CD and  $K_{sv} = 1.53 \times 10^2$  M $^{-1}$  at  $\lambda_{ex} = 295$  nm. (f) Quantum yield plots of BSA and ibuprofen at  $\lambda_{ex} = 295$  nm for various concentrations of  $\beta$ -CD and 2HP- $\beta$ -CD. The quantum yield of BSA and ibuprofen increases with the increase in [2HP- $\beta$ -CD], whereas there is a little decrease in quantum yield with the increase in [ $\beta$ -CD] (Figure S6). Interaction of BSA and oligosaccharides in the absence of ibuprofen.

with the increase in the concentration of surfactants. The  $\alpha$ -helix is found to decrease from 67.75 to 47.09% on addition of 0.1 mM CTAB, and on further increasing the concentration, the minima at 208 nm vanished, and consecutive negative and positive peaks are observed. On increasing the concentration of anionic surfactant SDS from 0 to 10 mM, the %  $\alpha$ -helix of 1  $\mu$ M BSA is found to decrease from 67.75 to 45.45%. The shift in the positions of the minima on rising the concentration of surfactants both in the presence and absence of the drug ibuprofen might be due to partial denaturation of the protein by the surfactant, leading to unfold the protein conformation, which allows the solvent molecules to interact with the electrons in the amino acids; as a result, the electronic states of the amino acids get destabilized and lead to shift in the peaks of amino acid absorption.<sup>47</sup>

When cationic (CTAB) and anionic (SDS) surfactants interact with the BSA and ibuprofen complex, their interactions lead to a change in the microenvironment of the tryptophan residue, which leads to a change in their exposure to solvent, as a consequence of which the quantum yield for

the BSA and ibuprofen complex alters. The quantum yield of the BSA Trp residue has been reported to be 0.14,<sup>54</sup> which has been taken as a standard. The quantum yield of BSA in the presence of ibuprofen at different concentrations of surfactants has been calculated by using the equation given by

$$\Phi_X = \Phi_{ST} \left( \frac{OD_{ST}}{OD_X} \right) \left( \frac{A_X}{A_{ST}} \right) \left( \frac{n_X^2}{n_{ST}^2} \right) \left( \frac{D_X}{D_{ST}} \right) \quad (8)$$

where  $\Phi_X$  = quantum yield of BSA in the presence of ibuprofen and surfactant,  $\Phi_{ST}$  = quantum yield of BSA (i.e., 0.14),  $OD_{ST}$  = optical density or absorbance of BSA,  $OD_X$  = optical density or absorbance of BSA in the presence of ibuprofen and surfactant,  $A_X$  = area under the fluorescence intensity curve of BSA in the presence of ibuprofen and surfactant,  $A_{ST}$  = fluorescence intensity of BSA,  $n_X$  = refractive index of BSA in the presence of ibuprofen and surfactant,  $n_{ST}$  = refractive index of the standard BSA,  $D_X$  = dilution ratio of BSA in the presence of ibuprofen and surfactant, and  $D_{ST}$  = dilution ratio of standard BSA.<sup>55</sup>  $n_X$  and  $n_{ST}$  are the same in our case, also  $D_X$

and  $D_{ST}$  are the same as samples for fluorescence spectrum measurement are not diluted. Therefore, the above equation can be rewritten as

$$\Phi_X = \Phi_{ST} \left( \frac{OD_{ST}}{OD_X} \right) \left( \frac{A_X}{A_{ST}} \right) \quad (9)$$

The quantum yield of BSA and ibuprofen in the presence of a different concentration of CTAB and SDS at  $\lambda_{ex} = 295$  nm and pH = 7.4 is shown in Figure 2g, but when the interaction of BSA and ibuprofen with different concentrations of SDS (from 0 to 15 mM) is observed, the quantum yield first decreases up to 1 mM and then increase linearly up to 8 mM (CMC of SDS) and then decreases post-CMC, whereas it is observed that when BSA interacts with CTAB/SDS in the absence of ibuprofen, the quantum yield decreases linearly with an increase in the concentration of both surfactants from 0 to 15 mM (Figure S4c).

To determine the quenching constants and stoichiometry, the Stern–Volmer equation<sup>56</sup> and double-logarithm Stern–Volmer (DLSV)<sup>36</sup> have been, respectively, used. The Stern–Volmer equation is given by

$$\frac{F_0 - F}{F} = K_{SV}[Q] \quad (10)$$

where  $F$  = fluorescence intensity of BSA and ibuprofen in the presence of surfactants,  $F_0$  = fluorescence intensity of BSA and ibuprofen in the absence of surfactants,  $[Q]$  = concentration of ibuprofen, and  $K_{SV}$  = quenching constant (also known as the Stern–Volmer constant). The value of  $K_{SV}$  is calculated from the slope of the graph of  $(F_0 - F)/F$  versus  $[Q]$  as shown in Figure S4d for both CTAB and SDS at  $\lambda_{ex} = 295$  nm. The  $K_{SV}$ s are determined to be  $8.684 \times 10^1 \text{ M}^{-1}$  for SDS and  $8.968 \times 10^1 \text{ M}^{-1}$  for CTAB.

To calculate the number of binding sites, double-logarithm Stern–Volmer (DLSV) is employed. The DLSV equation is given by

$$\log \left\{ \frac{F_0 - F}{F} \right\} = \log K_{SV} + n \log[Q] \quad (11)$$

where  $n$  = number of binding sites. The number of binding sites “ $n$ ” is obtained from the slope of the plot of  $\log \left\{ \frac{F_0 - F}{F} \right\}$  versus  $\log[Q]$  as shown in Figure 2h ( $\lambda_{ex} = 295$  nm). The number of binding sites in BSA in the presence of ibuprofen is found to be 1.146 and 0.998 for SDS and CTAB, respectively. The value of “ $n$ ” is nearly equal to 1 in both the cases, but the actual value of “ $n$ ” in the case of CTAB (cationic surfactant) is less as compared to SDS (anionic surfactant).

**3.3. Binding of Ibuprofen to BSA Decreases in the Presence of Oligosaccharides, but Solubility Increases by the Formation of Inclusion Complex.** The effect of oligosaccharides ( $\beta$ -CD and 2-HP- $\beta$ -CD) on the binding interaction of BSA and ibuprofen is studied by fluorescence spectroscopy at  $\lambda_{ex} = 295$  nm and pH = 7.4 as shown in Figure 3a,b, respectively. It is observed that as the concentration of  $\beta$ -CD and 2-HP- $\beta$ -CD increases, there is no significant decrease in the fluorescence intensity of BSA at around  $\lambda = 338$  nm, which indicates that there is no change in the microenvironment of BSA Trp-212; because of the large size of  $\beta$ -CD and 2-HP- $\beta$ -CD, they could not be able to approach the hydrophobic core of BSA where the tryptophan-212 residues and Trp-134 has a dilution effect on fluorescence quenching by  $\beta$ -CD<sup>56</sup> and

2-HP- $\beta$ -CD. Also, the dilution in the quenching of fluorescence intensity of BSA might be due to Trp-134, which is located at the surface of the protein.<sup>56</sup> However, the fluorescence intensity for ibuprofen (at  $\lambda_{em} = 350$  nm) increases with an increase in the concentration of  $\beta$ -CD/2-HP- $\beta$ -CD. This may be due to the formation of inclusion complexes between ibuprofen and  $\beta$ -CD/2-HP- $\beta$ -CD,<sup>57</sup> which lead to an increase in the solubility of ibuprofen.<sup>55</sup> To further support the fact that there is formation of inclusion complexes between ibuprofen and  $\beta$ -CD/2-HP- $\beta$ -CD, the interaction of ibuprofen with  $\beta$ -CD and 2-HP- $\beta$ -CD is analyzed with fluorescence emission spectroscopy at  $\lambda_{ex} = 295$  nm and pH = 7.4 (Figure S6a,b, respectively).<sup>58</sup> The increase in the fluorescence intensity of ibuprofen at  $\lambda_{em} = 355$  nm with the rise in the concentration of  $\beta$ -CD/2-HP- $\beta$ -CD implies that there is the formation of inclusion complexes which lead to an increase in fluorescence intensity as well as the solubility of the hydrophobic drug ibuprofen. The effect of oligosaccharides ( $\beta$ -CD and 2-HP- $\beta$ -CD) on the binding interaction of ibuprofen with BSA tryptophan and tyrosine residues at  $\lambda_{ex} = 275$  nm and pH = 7.4 is shown in Figure S6e,h, respectively. Similar observations are found at  $\lambda_{ex} = 275$  nm, as there is no significant quenching observed at  $\lambda_{em} = 338$  nm corresponding to BSA emission.

SFS (at  $\Delta\lambda = 35$  nm) is performed for BSA and ibuprofen at different concentrations of  $\beta$ -CD and 2-HP- $\beta$ -CD to study the change in the microenvironment of protein BSA on binding interaction with ibuprofen as shown in Figure 3c,d, respectively. It is observed that as the concentration of  $\beta$ -CD and 2-HP- $\beta$ -CD increases, the synchronous fluorescence intensity decreases for BSA at  $\lambda = 318$  nm, but the decrease is not significant, which supports the normal fluorescence emission data. There is an increase in the intensity of the two peaks at 364 and 353 nm corresponding to ibuprofen, but the increase is non-linear. This further supports the fact that with the rise in the concentration of  $\beta$ -CD or 2-HP- $\beta$ -CD, there is more probability of inclusion complex formation between ibuprofen and  $\beta$ -CD or 2-HP- $\beta$ -CD, which enhances the fluorescence intensity of the two SFS peaks corresponding to ibuprofen, but due to the large size of the inclusion complex, they are unable to interact with the Trp and Tyr residues of BSA. To further verify the fact that there is no significant change in the microenvironment of Tyr and Trp residues of BSA, synchronous data are also taken at  $\Delta\lambda = 15$  and 60 nm, respectively (Figure S6f,g and S6i,j, respectively, for  $\beta$ -CD and 2-HP- $\beta$ -CD). The peak 302 nm in SFS at  $\Delta\lambda = 15$  nm for both  $\beta$ -CD and 2-HP- $\beta$ -CD correspond to the Tyr residue of BSA. There is neither any peak shift nor any significant quenching in peak intensity with the rise in the concentrations of  $\beta$ -CD and 2-HP- $\beta$ -CD, but there is an increase in the SFS peak intensity corresponding to ibuprofen at 346 nm, which is consistent with the fluorescence emission data. Similar results are obtained in SFS  $\Delta\lambda = 60$  nm, where there is no change in SFS peak intensity at  $\lambda = 339$  nm corresponding to BSA Trp emission.

It is observed from the fluorescence emission data that the resultant fluorescence intensity corresponding to BSA (25  $\mu\text{M}$ ) and ibuprofen (25  $\mu\text{M}$ ) increases with an increase in the concentration of oligosaccharides, but there is no significant change in emission intensity at  $\lambda_{em} = 338$  nm (for BSA only). To determine the binding properties in the presence of oligosaccharides, a Benesi–Hildebrand equation is used. To find out the binding constant,  $1/(F - F_0)$  is plotted against  $1/[Q]$  as shown in Figure 3e. The respective  $K_{SV}$  value for BSA

and ibuprofen in the presence of  $\beta$ -CD and 2-HP- $\beta$ -CD at  $\lambda_{\text{ex}} = 295 \text{ nm}$  is calculated to be  $1.65103$  and  $1.53 \times 10^2 \text{ M}^{-1}$ , respectively. To evaluate the binding constants of the interaction of ibuprofen with  $\beta$ -CD and 2-HP- $\beta$ -CD and to investigate the behaviors of inclusion complexes, Benesi–Hildebrand eq 6 is used (Figure S6c,d). The binding constants of ibuprofen with  $\beta$ -CD and 2-HP- $\beta$ -CD are determined by using eq 7 and are obtained to be  $4.017 \times 10^2$  and  $5.873 \times 10^2 \text{ M}^{-1}$ , respectively. The above results imply that the binding interaction between ibuprofen and 2-HP- $\beta$ -CD in their inclusion complex is stronger than that of the ibuprofen- $\beta$ -CD inclusion complex.<sup>59</sup>

The quantum yields are calculated for BSA and ibuprofen in the presence of different concentrations of  $\beta$ -CD or 2-HP- $\beta$ -CD. As shown in Figure 3f, with an increase in the concentration of 2-HP- $\beta$ -CD, the quantum yield value increases, which is consistent with the fluorescence emission data as there is an increase in fluorescence intensity with the rise in the concentration of 2-HP- $\beta$ -CD. However, in the case of  $\beta$ -CD, the change in quantum yield is almost constant as it is observed that there is no significant increase in fluorescence intensity with an increase in the concentration of  $\beta$ -CD. However, for both  $\beta$ -CD and 2-HP- $\beta$ -CD, an increase in absorbance is observed with the increase in the concentrations of oligosaccharides with fixed concentrations of BSA ( $25 \mu\text{M}$ ) and ibuprofen ( $25 \mu\text{M}$ ) (Figure S6k,l).

**3.4. FRET from BSA (in the Presence of SDS) to Ibuprofen Confirms Ibuprofen Binding to BSA Even in the Partially Unfolded Conformation.** The FRET experiment is employed to calculate the distance between the donor ( $25 \mu\text{M}$  BSA in the presence of  $40 \text{ mM}$  SDS) and acceptor (ibuprofen) as FRET is a distance-dependent process and occurs due to the dynamic interaction between the donor and acceptor.<sup>60</sup> From the fluorescence energy transfer efficiency, the actual distance between the donor and acceptor is calculated by using eq 3. There are two important conditions for energy transfer to occur: (i) there must be a significant overlap between the emission spectra of the donor and the absorption spectra of the acceptor and (ii) the distance between the donor and acceptor should be  $\leq 10 \text{ nm}$ .<sup>34</sup>

The normalized overlap spectra between the donor emission and acceptor absorption along with acceptor emission and donor absorption are shown in Figure S7. To achieve a significant overlap between donor emission and acceptor absorption spectra, and to study the interaction of the drug (ibuprofen) in an unfolded (denatured) state of BSA, SDS is used. The overlap between donor emission spectra and acceptor absorption spectra is called an overlap integral " $J(\lambda)$ " and is calculated to be  $3.899 \times 10^{13} \text{ nm}^4 \text{ M}^{-1} \text{ cm}^{-1}$ . The  $J(\lambda)$  value thus obtained is used in eq 4 to calculate the Förster distance ( $R_0$ ) and is determined to be  $5.89 \text{ nm}$ . The fluorescence emission plots of only  $25 \mu\text{M}$  BSA in the presence of  $40 \text{ mM}$  SDS (donor), only  $10 \mu\text{M}$  ibuprofen (acceptor), and a mixture of both donor and acceptor are shown in Figure 4. It is observed that there is a decrease in the fluorescence intensity of the donor, whereas the acceptor's fluorescence intensity increases due to the Förster resonance energy transfer between the donor and acceptor. From eq 3, the energy-transfer efficiency ( $E$ ) is determined to be  $14\%$  with respect to acceptor rise, which is used to calculate the actual distance between the donor and acceptor ( $r$ ), and it is evaluated to be  $7.87 \text{ nm}$ , which is consistent with the condition that  $0.5 R_0 < r < 1.5 R_0$ <sup>61</sup> ( $2.945 < 7.87 < 8.835$ ). We have used acceptor rise over

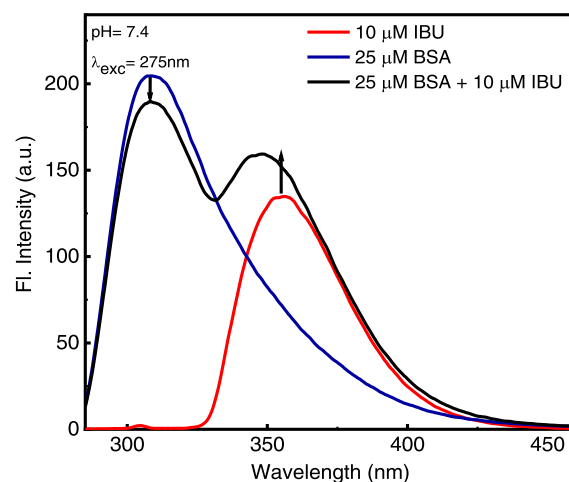


**Figure 4.** FRET study of  $25 \mu\text{M}$  BSA in the presence of  $40 \text{ mM}$  SDS (donor) and  $10 \mu\text{M}$  ibuprofen (acceptor) at  $\text{pH} = 7.4$  and  $\lambda_{\text{exc}} = 275 \text{ nm}$  confirms ibuprofen binding to BSA even in the partially unfolded conformation. The energy-transfer efficiency with respect to the acceptor is calculated to be  $14\%$  when the actual distance between donor and acceptor ( $r$ ) is obtained to be  $7.87 \text{ nm}$ . The overlap integral  $J(\lambda)$  is calculated to be  $3.899 \times 10^{13} \text{ nm}^4 \text{ M}^{-1} \text{ cm}^{-1}$ . These results imply that the drug ibuprofen is interacting with the tryptophan and tyrosine residues, and due to the high concentration of surfactant, the protein is unfolded, which decreases the energy-transfer efficiency as the distance between the protein and drug is  $7.87 \text{ nm}$ . Figure S7 shows an overlap of emission spectrum of BSA in the presence of SDS (donor) and absorption spectrum of ibuprofen (acceptor).

donor quenching for the calculation of FRET efficiency and the distance between the donor and acceptor because of the fact that quenching in the fluorescence intensity of the donor could be affected by a number of interactions such as reactions in the excited state, energy transfer to the acceptor, rearrangements at the molecular level, complex formation, and collision between the fluorophore and quencher, whereas a rise in the fluorescence intensity of the acceptor (here ibuprofen) will be mainly by transfer of energy from the donor.<sup>62</sup> The above results imply that there is a possibility of energy transfer between BSA in its partially unfolded state to ibuprofen, which further suggests that ibuprofen is bound to BSA in its partially unfolded conformation. Thus, BSA can also be used as a drug (ibuprofen) carrier even in its unfolded conformation as evident from the FRET study.

**3.5. 3D Fluorescence Spectral Analysis of Interaction of BSA and Ibuprofen Elucidates the Polarity Changes in the Protein BSA upon Ibuprofen Binding and Further Confirms the FRET from BSA to Ibuprofen in the Presence of Surfactants.** 3D fluorescence spectroscopy or total fluorescence spectroscopy is one of the powerful spectroscopic techniques used to investigate samples containing multiple fluorophores, which have overlapping emission spectra, and also to analyses drug–protein interaction,<sup>63</sup> and the corresponding 3D contour plots specifically provide information about the conformational changes in protein by binding with the drug molecule(s).<sup>64</sup>

The 3D contour plot for only  $25 \mu\text{M}$  BSA is shown in Figure Sa, which shows two peaks—one at  $\lambda_{\text{ex}} = 277 \text{ nm}$  and  $\lambda_{\text{em}} = 336 \text{ nm}$  ( $3.69 \text{ eV}$ ) (peak 1a) corresponding to aromatic residues (tryptophan, tyrosine, and phenylalanine) and another peak named as peak 1b at  $\lambda_{\text{ex}} = 234 \text{ nm}$  and  $\lambda_{\text{em}} = 336 \text{ nm}$

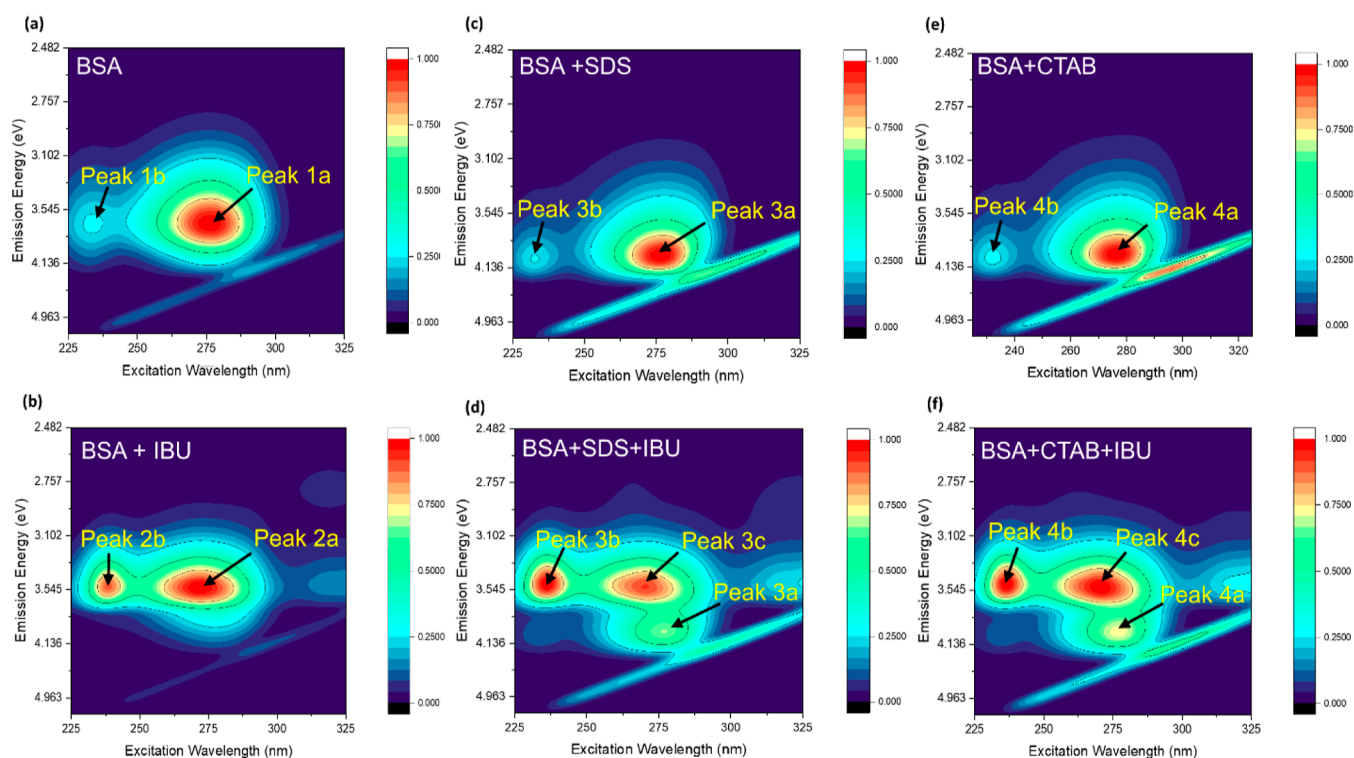


**Figure 5.** Normalized 3D fluorescence spectral analysis of interaction of BSA and ibuprofen at pH = 7.4 elucidates the polarity changes in the protein BSA upon ibuprofen binding and further confirms the FRET from BSA to ibuprofen in the presence of surfactants. (a,b) Represent 3D fluorescence contour plots of 25  $\mu\text{M}$  BSA (only) and 25  $\mu\text{M}$  BSA and 15  $\mu\text{M}$  ibuprofen, respectively. 25  $\mu\text{M}$  BSA shows two peaks: one at  $\lambda_{\text{ex}} = 277$  nm and  $\lambda_{\text{em}} = 336$  nm (3.69 eV) (peak 1a) and at  $\lambda_{\text{ex}} = 234$  nm and  $\lambda_{\text{em}} = 336$  nm (3.69 eV) (peak 1b) corresponding to normal and higher order excitation of aromatic residues, respectively, whereas the mixture (25  $\mu\text{M}$  BSA and 15  $\mu\text{M}$  ibuprofen) shows two peaks at  $\lambda_{\text{ex}} = 272$  nm (peak 2a) and at  $\lambda_{\text{ex}} = 238$  nm (peak 2b) and the corresponding emission at 355 nm. (c,d) 3D fluorescence contour plots of 25  $\mu\text{M}$  BSA and 40 mM SDS and 25  $\mu\text{M}$  BSA and 10  $\mu\text{M}$  ibuprofen in the presence of 40 mM SDS. The BSA and the SDS system shows two peaks: at  $\lambda_{\text{ex}} = 276$  nm (peak 3a) and at  $\lambda_{\text{ex}} = 232$  nm (peak 3b) and the corresponding maximum emission at 3.99 eV ( $\lambda_{\text{em}} = 311$  nm). BSA, SDS, and ibuprofen system shows three absorption maxima:  $\lambda_{\text{ex}} = 276$  nm ( $\lambda_{\text{em}} = 3.99$  eV) (peak 3a) corresponding to the BSA–SDS interaction peak,  $\lambda_{\text{ex}} = 236$  nm ( $\lambda_{\text{em}} = 355$  nm) (peak 3b) and  $\lambda_{\text{ex}} = 271$  nm ( $\lambda_{\text{em}} = 355$  nm) (peak 3c) refer to emission of ibuprofen by the binding interaction with BSA in the presence of SDS, corresponding to higher order and normal excitation, respectively. (e,f) 3D fluorescence contour plots of 25  $\mu\text{M}$  BSA and 40 mM CTAB and 25  $\mu\text{M}$  BSA and 10  $\mu\text{M}$  ibuprofen in the presence of 40 mM CTAB, respectively. BSA and CTAB system shows two peaks: peak 4a at  $\lambda_{\text{ex}} = 276$  nm and peak 4b at  $\lambda_{\text{ex}} = 232$  nm and corresponding emission at 3.99 eV, whereas BSA, CTAB, and ibuprofen system shows three peaks:  $\lambda_{\text{ex}} = 276$  nm ( $\lambda_{\text{em}} = 311$  nm) (peak 4a),  $\lambda_{\text{ex}} = 236$  nm ( $\lambda_{\text{em}} = 355$  nm) (peak 4b), and at  $\lambda_{\text{ex}} = 271$  nm ( $\lambda_{\text{em}} = 355$  nm) (peak 4c).

corresponding to higher excited-state excitation of aromatic amino acid residues of BSA.<sup>63</sup> The inclined contour surface in the 3D contour map where  $\lambda_{\text{ex}} = \lambda_{\text{em}}$  corresponds to Rayleigh scattering.<sup>65</sup> The 3D contour map of 15  $\mu\text{M}$  ibuprofen shows one prominent peak at  $\lambda_{\text{ex}} = 230$  nm (peak 1) corresponding to higher excited-state excitation and another peak at  $\lambda_{\text{ex}} = 267$  nm (peak 2) might be due to normal excitation, and emission is observed at 355 nm (3.50 eV) (Figure S8). The 3D contour map to show the change in conformational change of BSA upon binding with 15  $\mu\text{M}$  ibuprofen is shown in Figure 5b, which shows two peaks at  $\lambda_{\text{ex}} = 272$  nm (peak 2a) and at  $\lambda_{\text{ex}} = 238$  nm (peak 2b), the overall peak intensity due to the binding interaction of BSA and ibuprofen gets red-shifted as ibuprofen shows emission maximum at 355 nm. The red shift of overall emission is in accordance with 2D fluorescence data. Furthermore, the prominence of peak 2b corresponding to higher excited-state excitation might be attributed to an increase in the probability of higher order excitation, facilitated by the interaction of ibuprofen.

The bird-eye-view of conformational changes in BSA by interaction with surfactants (anionic SDS and cationic CTAB) and their effect on the binding of ibuprofen to BSA are studied, and the corresponding 3D contour plots are shown in Figure

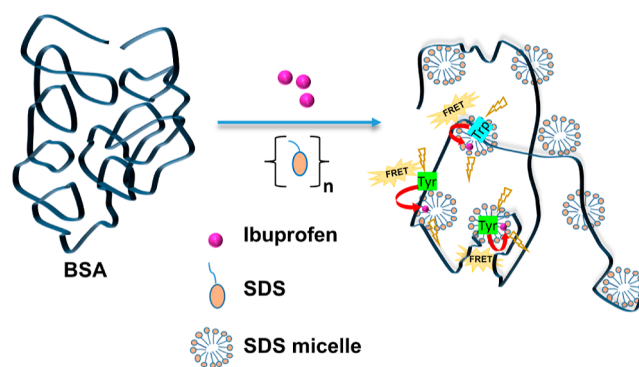
5c–f for an anionic surfactant (SDS) and its effect on the conformational change of BSA in the absence and presence of ibuprofen as shown in Figure 5c,d, respectively. Figure 5c shows one prominent peak at  $\lambda_{\text{ex}} = 276$  nm (peak 3a) and another peak at  $\lambda_{\text{ex}} = 232$  nm (peak 3b) and the corresponding emission for both the peaks at 311 nm (3.99 eV). The blue shift in the emission maxima of BSA from 336 nm (3.69 eV) (peak 1a of Figure 5a) to 311 nm (3.99 eV) (peak 3a of Figure 5c) in the presence of 40 mM SDS is clearly observed. This observation further supports the normal fluorescence data and is due to an increase in hydrophobicity around Trp-212 by the SDS micelle's hydrophobic core. The 3D contour plot of 25  $\mu\text{M}$  BSA in the presence of 10  $\mu\text{M}$  ibuprofen and 40 mM SDS as shown in Figure 5d shows three peaks:  $\lambda_{\text{ex}} = 276$  nm ( $\lambda_{\text{em}} = 311$  nm) (peak 3a) refers to the BSA–SDS interaction peak as explained before and  $\lambda_{\text{ex}} = 236$  nm ( $\lambda_{\text{em}} = 355$  nm) (peak 3b) and  $\lambda_{\text{ex}} = 271$  nm ( $\lambda_{\text{em}} = 355$  nm) (peak 3c) refer to the emission of ibuprofen by the binding interaction with BSA in the presence of SDS, corresponding to higher order and normal excitation, respectively. The blue shift and quenching in fluorescence intensity in emission peak 3a, corresponding to BSA in Figure 5d, are clear indications of a decrease in polarity around the microenvironments of aromatic amino acid

residues and unfolding of protein by the surfactant. Also, in Figure 5d, the dramatic increase in the intensity of the ibuprofen peak 3c compared to peak 2 of ibuprofen in Figure S8 and quenching of BSA peak 3a (at  $\lambda_{\text{ex}} = 276 \text{ nm}$  ( $\lambda_{\text{em}} = 311 \text{ nm}$ )) due to the interaction with BSA and SDS clearly indicates FRET from BSA to ibuprofen, which further supports the FRET experiment and also confirms that there is the binding of ibuprofen with BSA even in its partially denatured state.

Similarly, the change in the conformational states of BSA ( $25 \mu\text{M}$ ) in the presence of the cationic surfactant CTAB ( $40 \text{ mM}$ ) is shown in the 3D contour plot in Figure 5e, which shows two peaks named as peak 4a (at  $\lambda_{\text{ex}} = 276 \text{ nm}$  ( $\lambda_{\text{em}} = 311 \text{ nm}$ )) and 4b (at  $\lambda_{\text{ex}} = 232 \text{ nm}$  ( $\lambda_{\text{em}} = 311 \text{ nm}$ )) like BSA in the presence of SDS. The blue shift in emission maxima and the decrease in intensity are due to an increase in hydrophobicity around the microenvironments of aromatic amino acid residues by the CTAB micelle core and unfolding of the protein, which are consistent with the normal fluorescence emission. Figure 5f shows the 3D contour plot of BSA ( $25 \mu\text{M}$ ) and ibuprofen ( $15 \mu\text{M}$ ) in the presence of CTAB ( $40 \text{ mM}$ ). Like in the case of SDS, three peaks are observed: peak 4a at  $\lambda_{\text{ex}} = 276 \text{ nm}$  ( $\lambda_{\text{em}} = 311 \text{ nm}$ ), peak 4b at  $\lambda_{\text{ex}} = 236 \text{ nm}$  ( $\lambda_{\text{em}} = 355 \text{ nm}$ ), and peak 4c at  $\lambda_{\text{ex}} = 271 \text{ nm}$  ( $\lambda_{\text{em}} = 355 \text{ nm}$ ). The ibuprofen peak 4c gets enhanced and the BSA peak 4a gets quenched, indicating FRET from BSA to ibuprofen in the presence of CTAB, which imply that even in the partially unfolded state, there is binding interaction between ibuprofen and BSA. However, the quenching in the BSA peak is lesser as observed in the case of SDS.

In the final discussion, quenching of the BSA peak with the addition of ibuprofen clearly indicates their interaction as shown in Figure 1, but the overall increase in fluorescence emission and the red shift in emission maxima are due to the ibuprofen emission, and it should not be confused with the polarity change in the protein due to the interaction with ibuprofen. Both SDS and CTAB are found to partially unfold the protein structure and increase the hydrophobicity around the Tyr and Trp residues by either encapsulating the Trp and Tyr residues inside the micelles or by inducing self-coiling in the protein around the micelles, which is in accordance with the “necklace and bead structures” model as reported by Turro et al.<sup>66</sup> Cationic CTAB is found to interact with the negatively charged BSA extensively by electrostatic interactions and hence blue shifting the emission spectra and decreasing the  $\alpha$ -helix content of the protein significantly as observed in the CD plots (Figure S5b). SDS having an anionic head group could not be able to interact with the negatively charged BSA directly and remain away, but the non-polar tail interacts directly with the protein, leading to quenching in intrinsic protein fluorescence.<sup>3</sup> Above CMC, the micelles of SDS partially unfold the protein, and at this state, the interaction occurs leading to a blue shift and quenching in emission maxima. Figure 2 depicts the fact that ibuprofen can bind to BSA even in its partially unfolded state induced by CTAB or SDS. Based on the above observations, we proposed a model in Scheme 1 to show the non-radiative fluorescence energy transfer from Trp and Tyr residues of BSA to ibuprofen in the presence of SDS, which further supports the hydrophobic drug ibuprofen binding to BSA even in partially unfolded conformation (Figure 5). The binding of ibuprofen to the partially unfolded BSA can be understood by considering the protein–surfactant interaction by taking into account two possible “necklace and bead

**Scheme 1. Schematic Representation of FRET from Trp and Tyr Residues of BSA in the Presence of SDS to Ibuprofen**



structures” as proposed by Turro et al., (i) where partially unfolded BSA chain with Trp and Tyr residues wrapped by the SDS micelle interacts with ibuprofen and transfer their resonance energy to it and (ii) where the partially unfolded BSA chain self-coiled around the SDS micelle with Trp and Tyr residues transfer the resonance energy to ibuprofen by binding with it after the CMC.

#### 4. CONCLUSIONS

The current study clearly provides some important insights into the binding interaction of hydrophobic drug ibuprofen with BSA, in both its native and partially denatured conformation. The effect of pH, oligosaccharides ( $\beta$ -CD and 2-HP- $\beta$ -CD), and surfactants (SDS and CTAB) on the interaction of BSA and ibuprofen are also investigated. The results obtained from molecular docking analysis clearly indicate that ibuprofen can effectively bind to hydrophobic binding pockets in binding site II which is at subdomain IIIA of BSA. Like other NSAIDs, the major forces responsible for the binding interaction of ibuprofen with BSA are hydrophobic forces, hydrogen bonding interactions, and electrostatic interactions. The change in the microenvironment of Trp-212 by interaction with ibuprofen is clearly indicated by the blue shift in BSA emission in both normal fluorescence experiments and SFS at  $\Delta\lambda = 60 \text{ nm}$ . The result is further supported by 3D fluorescence plots. The BSA secondary structure upon binding with ibuprofen is found to be changed. The effect of different pH does not play any significant role in the binding of ibuprofen to BSA. The binding of ibuprofen with BSA is found to be possible even in its partially unfolded conformation, and during their interaction, there is FRET from BSA to ibuprofen, and the distance between denatured BSA and ibuprofen is calculated to be  $7.87 \text{ nm}$ . Oligosaccharides are forming inclusion complexes with ibuprofen due to hydrophobic interactions, thereby the solubility of the drug increases, but due to the bigger size of the drug–oligosaccharide inclusion complex, they are unable to interact with BSA. Ultimately, this investigation leads to the understanding of not only the mechanism of drug loading and transportation but also the effect of drugs on protein’s conformation during these processes. The study could provide some valuable insights into the mechanism of loading and transportation of other NSAIDs to BSA and could be extended to HSA as both are homologous to each other. However, in vivo experiments using appropriate mouse models need to be conducted to get detailed mechanism of such interactions as in

vitro measurements could not mimic the complex in vivo atmosphere.

## ■ ASSOCIATED CONTENT

### SI Supporting Information

The Supporting Information is available free of charge at <https://pubs.acs.org/doi/10.1021/acsomega.2c06447>.

Fluorescence spectra, synchronous fluorescence spectra, and maximum wavelength versus concentration plots of BSA and ibuprofen at pH = 7.4, 6.5, and 8 and in the presence and absence of surfactants (CTAB and SDS) and oligosaccharides ( $\beta$ -CD and 2-HP- $\beta$ -CD) along with the  $^1\text{H}$  NMR spectra of ibuprofen in the presence and absence of BSA, CD spectra of BSA at pH = 6.5 and 8, and with different concentrations of SDS and CTAB in the absence of ibuprofen, and 3D fluorescence spectra of ibuprofen, absorbance, Stern–Volmer, Benesi–Hildebrand, and quantum yield plots (PDF)

## ■ AUTHOR INFORMATION

### Corresponding Author

Dibyendu K. Sasmal – Department of Chemistry, Indian Institute of Technology, Jodhpur, Rajasthan 342037, India;  
orcid.org/0000-0003-4148-5326; Phone: (+91)-291-280-1314; Email: [sasmal@iitj.ac.in](mailto:sasmal@iitj.ac.in); [www.sasmallab.org](http://www.sasmallab.org)

### Authors

Debashish Rout – Department of Chemistry, Indian Institute of Technology, Jodhpur, Rajasthan 342037, India  
Shweta Sharma – Department of Chemistry, Indian Institute of Technology, Jodhpur, Rajasthan 342037, India  
Pratibha Agarwala – Department of Chemistry, Indian Institute of Technology, Jodhpur, Rajasthan 342037, India  
Arun K. Upadhyaya – Department of Chemistry, Indian Institute of Technology, Jodhpur, Rajasthan 342037, India  
Akanksha Sharma – Department of Chemistry, Indian Institute of Technology, Jodhpur, Rajasthan 342037, India

Complete contact information is available at:  
<https://pubs.acs.org/10.1021/acsomega.2c06447>

### Notes

The authors declare no competing financial interest.

## ■ ACKNOWLEDGMENTS

We would like to thank SERB, Department of Science and Technology for Start-up Research Grant (grant number—SRG/2020/001730). We also like to thank IIT Jodhpur for the SEED grant. D.R., S.S., P.A., and A.K.U. thank to IIT Jodhpur for fellowship. A.S. thank to CSIR for fellowship. D.K.S. and all other authors thank the Department of Chemistry and CASE for providing instrument facility.

## ■ REFERENCES

- (1) Tayyab, S.; Feroz, S. R. Serum Albumin: Clinical Significance of Drug Binding and Development as Drug Delivery Vehicle. *Adv. Protein Chem. Struct. Biol.* **2021**, *123*, 193–218.
- (2) Glassman, P. M.; Muzykantov, V. R. Pharmacokinetic and Pharmacodynamic Properties of Drug Delivery Systems. *J. Pharmacol. Exp. Ther.* **2019**, *370*, S70–S80.
- (3) Agarwala, P.; Bera, T.; Sasmal, D. K. Molecular Mechanism of Interaction of Curcumin with BSA, Surfactants and Live *E. Coli* Cell Membrane Revealed by Fluorescence Spectroscopy and Confocal Microscopy. *ChemPhysChem* **2022**, *23*, No. e202200265.
- (4) Du, X.; Li, Y.; Xia, Y. L.; Ai, S. M.; Liang, J.; Sang, P.; Ji, X. L.; Liu, S. Q. Insights into Protein–Ligand Interactions: Mechanisms, Models, and Methods. *Int. J. Mol. Sci.* **2016**, *17*, 144.
- (5) Yang, J.; Roy, A.; Zhang, Y. Protein-Ligand Binding Site Recognition Using Complementary Binding-Specific Substructure Comparison and Sequence Profile Alignment. *Bioinformatics* **2013**, *29*, 2588–2595.
- (6) Tesseromatis, C.; Alevizou, A. The Role of the Protein-Binding on the Mode of Drug Action as Well the Interactions with Other Drugs. *Eur. J. Drug Metab. Pharmacokinet.* **2008**, *33*, 225.
- (7) Hansda, C.; Maiti, P.; Singha, T.; Pal, M.; Hussain, S. A.; Paul, S.; Paul, P. K. Photophysical Study of the Interaction between ZnO Nanoparticles and Globular Protein Bovine Serum Albumin in Solution and in a Layer-by-Layer Self-Assembled Film. *J. Phys. Chem. Solids* **2018**, *121*, 110–120.
- (8) Lu, R.; Li, W. W.; Katzir, A.; Raichlin, Y.; Yu, H. Q.; Mizaikoff, B. Probing the Secondary Structure of Bovine Serum Albumin during Heat-Induced Denaturation Using Mid-Infrared Fiber Optic Sensors. *Analyst* **2015**, *140*, 765–770.
- (9) Fologea, D.; Ledden, B.; McNabb, D. S.; Li, J. Electrical Characterization of Protein Molecules by a Solid-State Nanopore. *Appl. Phys. Lett.* **2007**, *91*, 053901.
- (10) Belinskaia, D. A.; Voronina, P. A.; Shmurak, V. I.; Jenkins, R. O.; Goncharov, N. V. Serum Albumin in Health and Disease: Esterase, Antioxidant, Transporting and Signaling Properties. *Int. J. Mol. Sci.* **2021**, *22*, 10318.
- (11) Chaves, O. A.; Vazquez, L. Molecular Docking Analysis on the Interaction between Bovine Serum Albumin and Three Commercial Fluoroquinolones: Ciprofloxacin, Enrofloxacin and Pefloxacin. *Eur. J. Chem.* **2021**, *12*, 192–196.
- (12) Sengupta, P.; Sardar, P. S.; Roy, P.; Dasgupta, S.; Bose, A. Investigation on the Interaction of Rutin with Serum Albumins: Insights from Spectroscopic and Molecular Docking Techniques. *J. Photochem. Photobiol., B* **2018**, *183*, 101–110.
- (13) Cheng, Z. J.; Zhao, H. M.; Xu, Q. Y.; Liu, R. Investigation of the Interaction between Indigotin and Two Serum Albumins by Spectroscopic Approaches. *J. Pharm. Anal.* **2013**, *3*, 257–269.
- (14) Chudzik, M.; Maciązek-Jurczyk, M.; Pawelczak, B.; Sulowska, A. Spectroscopic Studies on the Molecular Ageing of Serum Albumin. *Molecules* **2017**, *22*, 34.
- (15) Starosta, R.; Santos, F. C.; de Almeida, R. F. M. Human and Bovine Serum Albumin Time-Resolved Fluorescence: Tryptophan and Tyrosine Contributions, Effect of DMSO and Rotational Diffusion. *J. Mol. Struct.* **2020**, *1221*, 128805.
- (16) Anand, U.; Jash, C.; Boddepalli, R. K.; Shrivastava, A.; Mukherjee, S. Exploring the Mechanism of Fluorescence Quenching in Proteins Induced by Tetracycline. *J. Phys. Chem. B* **2011**, *115*, 6312–6320.
- (17) Gelamo, E. L.; Silva, C. H. T. P.; Imasato, H.; Tabak, M. Interaction of Bovine (BSA) and Human (HSA) Serum Albumins with Ionic Surfactants: Spectroscopy and Modelling. *Biochim. Biophys. Acta, Protein Struct. Mol. Enzymol.* **2002**, *1594*, 84–99.
- (18) Varga, Z.; Sabzwariali, S. R.; Vargova, V. Cardiovascular Risk of Nonsteroidal Anti-Inflammatory Drugs: An Under-Recognized Public Health Issue. *Cureus* **2017**, *9*, No. e1144.
- (19) Pereira-Leite, C.; Nunes, C.; Reis, S. Interaction of nonsteroidal anti-inflammatory drugs with membranes: In vitro assessment and relevance for their biological actions. *Prog. Lipid Res.* **2013**, *52*, 571–584.
- (20) Varrassi, G.; Pergolizzi, J. V.; Dowling, P.; Paladini, A. Ibuprofen Safety at the Golden Anniversary: Are All NSAIDs the Same? A Narrative Review. *Adv. Ther.* **2020**, *37*, 61–82.
- (21) Evans, A. M. Comparative Pharmacology of S(+)-Ibuprofen and (R)-Ibuprofen. *Clin. Rheumatol.* **2001**, *20*, S9–S14.
- (22) Mazaleuskaya, L. L.; Theken, K. N.; Gong, L.; Thorn, C. F.; FitzGerald, G. A.; Altman, R. B.; Klein, T. E. PharmGKB Summary: Ibuprofen Pathways. *Pharmacogenet. Genomics* **2015**, *25*, 96–106.
- (23) Bushra, R.; Aslam, N. An Overview of Clinical Pharmacology of Ibuprofen. *Oman Med. J.* **2010**, *25*, 155–166.

- (24) Tiwari, G.; Tiwari, R.; Rai, A. Cyclodextrins in Delivery Systems: Applications. *J. Pharm. BioAllied Sci.* **2010**, *2*, 72.
- (25) Thi, T. D.; Nauwelaerts, K.; Baudemprez, L.; van Speybroeck, M.; Vermant, J.; Augustijns, P.; Annaert, P.; Martens, J.; van Humbeeck, J.; van den Mooter, G. Comparison between 2-Hydroxypropyl- $\beta$ -Cyclodextrin and 2-Hydroxypropyl- $\gamma$ -Cyclodextrin for Inclusion Complex Formation with Danazol. *J. Inclusion Phenom. Macrocyclic Chem.* **2011**, *71*, 137–147.
- (26) Pereva, S.; Sarafska, T.; Bogdanova, S.; Spassov, T. Efficiency of “Cyclodextrin-Ibuprofen” Inclusion Complex Formation. *J. Drug Delivery Sci. Technol.* **2016**, *35*, 34–39.
- (27) Saokham, P.; Muankaew, C.; Jansook, P.; Loftsson, T. Solubility of Cyclodextrins and Drug/Cyclodextrin Complexes. *Molecules* **2018**, *23*, 1161.
- (28) Yuan, C.; Jin, Z.; Li, X. Evaluation of Complex Forming Ability of Hydroxypropyl- $\beta$ -Cyclodextrins. *Food Chem.* **2008**, *106*, 50–55.
- (29) Kumar, A.; Khan, A.; Janakiraman, A. K. Surfactants and Their Role in Pharmaceutical Product Development: An Overview. *J. Pharm. Pharm.* **2019**, *6*, 72–82.
- (30) Vlasova, I. M.; Zhuravleva, V. v.; Vlasov, A. A.; Saletsky, A. M. Interaction of Cationic Surfactant Cetyltrimethylammonium Bromide with Bovine Serum Albumin in Dependence on pH: A Study of Tryptophan Fluorescence. *J. Mol. Struct.* **2013**, *1034*, 89–94.
- (31) Singh, V.; Tyagi, R. Investigations of Mixed Surfactant Systems of Lauryl Alcohol-Based Bissulfosuccinate Anionic Gemini Surfactants with Conventional Surfactants: A Fluorometric Study. *J. Taibah Univ. Sci.* **2015**, *9*, 477–489.
- (32) Morales, P.; Williams. Reviewl.
- (33) Kumar Padhy, R. Estimation of Ibuprofen Solubilization in Cationic and Anionic Surfactant Media: Application of Micelle Binding Model. *Indian J. Chem. Technol.* **2009**, *16*, 426–430.
- (34) Sasmal, D. K.; Pulido, L. E.; Kasal, S.; Huang, J. Single-Molecule Fluorescence Resonance Energy Transfer in Molecular Biology. *Nanoscale* **2016**, *28*, 19928–19944.
- (35) Khodarahmi, R.; Karimi, S. A.; Ashrafi Kooshk, M. R.; Ghadami, S. A.; Ghobadi, S.; Amani, M. Comparative Spectroscopic Studies on Drug Binding Characteristics and Protein Surface Hydrophobicity of Native and Modified Forms of Bovine Serum Albumin: Possible Relevance to Change in Protein Structure/Function upon Non-Enzymatic Glycation. *Spectrochim. Acta, Part A* **2012**, *89*, 177–186.
- (36) Amézqueta, S.; Beltrán, J. L.; Bolioli, A. M.; Campos-vicens, L.; Luque, F. J.; Ràfols, C. Evaluation of the Interactions between Human Serum Albumin (Hsa) and Non-steroidal Anti-inflammatory (Nsaid) Drugs by Multiwavelength Molecular Fluorescence, Structural and Computational Analysis. *Pharmaceuticals* **2021**, *14*, 214.
- (37) Hospes, M.; Hendriks, J.; Hellingwerf, K. J. Tryptophan Fluorescence as a Reporter for Structural Changes in Photoactive Yellow Protein Elicited by Photo-Activation. *Photochem. Photobiol. Sci.* **2013**, *12*, 479–488.
- (38) Meti, M. D.; Nandibewoor, S. T.; Joshi, S. D.; More, U. A.; Chimatar, S. A. Binding Interaction and Conformational Changes of Human Serum Albumin with Ranitidine Studied by Spectroscopic and Time-Resolved Fluorescence Methods. *J. Iran. Chem. Soc.* **2016**, *13*, 1325–1338.
- (39) Xu, H.; Yao, N.; Xu, H.; Wang, T.; Li, G.; Li, Z. Characterization of the Interaction between Eupatorin and Bovine Serum Albumin by Spectroscopic and Molecular Modeling Methods. *Int. J. Mol. Sci.* **2013**, *14*, 14185–14203.
- (40) Magdy, G.; Belal, F.; Abdel-Megied, A. M.; Hakiem, A. F. A. Two Different Synchronous Spectrofluorimetric Approaches for Simultaneous Determination of Febuxostat and Ibuprofen. *R. Soc. Open Sci.* **2021**, *21*, 210354.
- (41) Al-Mehizia, A. A.; Bakheit, A. H.; Zargar, S.; Bhat, M. A.; Asmari, M. M.; Wani, T. A. Evaluation of Biophysical Interaction between Newly Synthesized Pyrazoline Pyridazine Derivative and Bovine Serum Albumin by Spectroscopic and Molecular Docking Studies. *J. Spectrosc.* **2019**, *2019*, 3848670.
- (42) Tian, J.; Zhao, Y.; Liu, X.; Zhao, S. A Steady-State and Time-Resolved Fluorescence, Circular Dichroism Study on the Binding of Myricetin to Bovine Serum Albumin. *Luminescence* **2009**, *24*, 386–393.
- (43) Wani, T. A.; Bakheit, A. H.; Ansari, M. N.; Al-Majed, A. R. A.; AlQahtani, B. M.; Zargar, S. Spectroscopic and Molecular Modeling Studies of Binding Interaction between Bovine Serum Albumin and Roflumilast. *Drug Des., Dev. Ther.* **2018**, *12*, 2627–2634.
- (44) Wang, H.; Fang, G.; Wang, H.; Dou, J.; Bian, Z.; Li, Y.; Chai, H.; Wu, Z.; Yao, Q. A Diboronic Acid Fluorescent Sensor for Selective Recognition of D-Ribose via Fluorescence Quenching. *New J. Chem.* **2019**, *43*, 4385–4390.
- (45) Punith, R.; Hegde, A. H.; Jaldappagari, S. Binding of an Anti-Inflammatory Drug Lornoxicam with Blood Proteins: Insights from Spectroscopic Investigations. *J. Fluoresc.* **2011**, *21*, 487–495.
- (46) Suganthi, M.; Elango, K. P. Synthesis, characterization and serum albumin binding studies of vitamin K3 derivatives. *J. Photochem. Photobiol., B* **2017**, *166*, 126–135.
- (47) Baral, A.; Satish, L.; Das, D. P.; Sahoo, H.; Ghosh, M. K. Construing the Interactions between MnO<sub>2</sub> Nanoparticle and Bovine Serum Albumin: Insight into the Structure and Stability of a Protein-Nanoparticle Complex. *New J. Chem.* **2017**, *41*, 8130–8139.
- (48) Krzyżak, E.; Szkatuła, D.; Wiatrak, B.; Gębarowski, T.; Marciniak, A. Synthesis, Cyclooxygenases Inhibition Activities and Interactions with BSA of N-Substituted 1H-Pyrrolo[3,4-c]Pyridine-1,3(2H)-Diones Derivatives. *Molecules* **2020**, *25*, 2934.
- (49) Ji, Z.; Yuan, H.; Liu, M.; Hu, J. <sup>1</sup>H-NMR Study of the Effect of Acetonitrile on the Interaction of Ibuprofen with Human Serum Albumin. *J. Pharm. Biomed. Anal.* **2002**, *30*, 151–159.
- (50) Luo, R.-S.; Liu, M.-L.; Mao, X.-A. NMR Diffusion and Relaxation Study on Ibuprofen—HSA Interaction. *Appl. Spectrosc.* **1999**, *53*, 776–779.
- (51) Bahri, M. A.; Hoebeke, M.; Grammenos, A.; Delanaye, L.; Vandewalle, N.; Seret, A. Investigation of SDS, DTAB and CTAB Micelle Microviscosities by Electron Spin Resonance. *Colloids Surf., A* **2006**, *290*, 206–212.
- (52) Ghisaidoobe, A. B. T.; Chung, S. J. Intrinsic Tryptophan Fluorescence in the Detection and Analysis of Proteins: A Focus on Förster Resonance Energy Transfer Techniques. *Int. J. Mol. Sci.* **2014**, *15*, 22518–22538.
- (53) Majumdar, T.; Bhowmik, D.; Kundu, A.; Dasmandal, S.; Mahapatra, A. The Effect of Serum Albumin, Surfactant and Their Mixture on the Reduction of a Cobalt(III) Complex by Ascorbic Acid. *Colloids Surf., A* **2013**, *436*, 185–192.
- (54) Chen, R. F. Fluorescence Quantum Yields of Tryptophan and Tyrosine. *Anal. Lett.* **1967**, *1*, 35–42.
- (55) *Application EBook Fluorescence Spectroscopy Fluorescence Spectroscopy 2*; JASCO Global, 2021.
- (56) Ghosh, S.; Kumar Paul, B.; Chattopadhyay, N. Interaction of Cyclodextrins with Human and Bovine Serum Albumins: A Combined Spectroscopic and Computational Investigation. *J. Chem. Sci.* **2014**, *126*, 931–944.
- (57) Gieroba, B.; Kalisz, G.; Sroka-Bartnicka, A.; Płazińska, A.; Płaziński, W.; Starek, M.; Abrowska, M. Molecular Structure of Cefuroxime Axetil Complexes with  $\alpha$ -,  $\beta$ -,  $\gamma$ -, and 2-Hydroxypropyl- $\beta$ -Cyclodextrins: Molecular Simulations and Raman Spectroscopic and Imaging Studies. *Int. J. Mol. Sci.* **2021**, *22*, 5238.
- (58) Laza-Knoerr, A. L.; Gref, R.; Couvreur, P. Cyclodextrins for Drug Delivery. *J. Drug Targeting* **2010**, *18*, 645–656.
- (59) Song, L. T.; Jiang, X. Y.; Tang, K. W.; Miao, J. B. Study on Inclusion Interaction of Ibuprofen with B-Cyclodextrin Derivatives. *Lat. Am. Appl. Res.* **2011**, *41*, 147–151.
- (60) Banerjee, P.; Ghosh, S.; Sarkar, A.; Bhattacharya, S. C. Fluorescence Resonance Energy Transfer: A Promising Tool for Investigation of the Interaction between 1-Anthracene Sulphonate and Serum Albumins. *J. Lumin.* **2011**, *131*, 316–321.
- (61) Ma, L.; Yang, F.; Zheng, J. Application of Fluorescence Resonance Energy Transfer in Protein Studies. *J. Mol. Struct.* **2014**, *1077*, 87–100.

- (62) Lakowicz, J. R. *Principles of Fluorescence Spectroscopy*; Springer, 2006.
- (63) Bortolotti, A.; Wong, Y. H.; Korsholm, S. S.; Bahring, N. H. B.; Bobone, S.; Tayyab, S.; van de Weert, M.; Stella, L. On the Purported “Backbone Fluorescence” in Protein Three-Dimensional Fluorescence Spectra. *RSC Adv.* **2016**, *6*, 112870–112876.
- (64) Wani, T. A.; Bakheit, A. H.; Abounassif, M. A.; Zargar, S. Study of Interactions of an Anticancer Drug Neratinib with Bovine Serum Albumin: Spectroscopic and Molecular Docking Approach. *Front. Chem.* **2018**, *6*, 47.
- (65) Buddanavar, A. T.; Nandibewoor, S. T. Multi-Spectroscopic Characterization of Bovine Serum Albumin upon Interaction with Atomoxetine. *J. Pharm. Anal.* **2017**, *7*, 148–155.
- (66) Turro, N. J.; Lei, X.-G.; Ananthpadmanabhan, K. P.; Aronson, M. Spectroscopic Probe Analysis of Protein-Surfactant Interactions: The BSA/SDS System. *Langmuir* **1995**, *11*, 2525–2533.